AD 746278

Semiannual Technical Report

Title: Noncrystalline Semiconductors: Electrical and Thermal Processes

ARPA Order No. 1562, Amend No. 1

Grant No. DA-ARO-D-31-124-72-G72

Program Code No. 61101D

Principal Investigator and Project Scientist:

Lyle H. Slack
(703) 552-6777

Effective Date of Grant: 1 January 1972

Expiration Date: 31 December 1972

Date of Report: 1 April 1972

Amount of Grant: $20,000

DDC
RECEIVED
AUG 7 1972
D.

# NONCRYSTALLINE SEMICONDUCTORS: ELECTRICAL
# AND THERMAL PROCESSES

## I.   Introduction

This project has two related objectives:

1.  To compare the actual switching behavior of amorphous semiconductor
    thin films with computer simulations of switching based on an
    assumed thermal mechanism.

2.  To apply electron spectroscopy to a basic understanding of electrical
    conduction in amorphous semiconductors.

During this first six months, the high speed switching in amorphous AsTe
was characterized as discussed in Section II. Digital computer simulations of
the Joule heating and heat transfer processes in amorphous semiconductor
switches have been carried out, and are described in Section III. The ESCA
(Electron Spectroscopy for Chemical Analysis) equipment with an associated
computer was installed and our initial studies on amorphous semiconductors
using this technique are described in Section IV.

## II.   Experimental Studies of Switching

An experimental study of switching in thin films of AsTe was undertaken
with Dr. S. A. Kostylev, an exchange scientist* from the Soviet Union.  A
publication[1] has been prepared on this initial work, in collaboration with
others, and is attached to this report.  The portions of that work which
are most pertinent to the computer simulation work are summarized here.

---

*Dr. Kostylev was a participant in the exchange scientist program between the
National Academy of Sciences and the Soviet Academy of Sciences.  He spent
three months here and three months at Wayne State University with M. P. Shaw.

AsTe glass was deposited on a brass plate by electron beam evaporation. The films studied had a thickness of $2\mu$m. Electrical experiments were performed under pulsed d.c. operation with pulse widths $t_p$ from 0.1 to $10\mu$ sec applied at a rate of 50-100 hz. In a given experiment the "sample" was considered to be the region of film in the immediate vicinity of the brass counter electrode, which had a tip about $200\mu$m wide at the point of contact.

Two distinctly different types of switching were usually observed. The usual delay-time switch was always observed in which the delay time decreased as the pulse applied voltage was increased above some critical voltage need for delay-time switching. The conductance of the film changes by a factor of $10^3$ during each delay-time switch. This event was usually preceeded by a "minor" switch which had essentially no delay time (less than a few nanoseconds) and involved only a five-fold conductance rise. The minor switch was often accompanied by relaxation oscillations at frequencies as high as 30M hz. The results indicate that the minor switch is electronic in nature but is not a necessary precursor to the delay-time switch. Delay-time switching can be made to occur at voltages lower than those for minor switching by heating the sample slightly above ambient.

The current rise during delay-time switching was found to follow a two power law

$$I = At^n + Bt^m$$

where $I$ = current,

$t$ = time, and

$A$, $B$, $n$, $m$ are experimental constants

A typical delay time for switching in the $2\mu$m AsTe film is between 1 and $10\mu$ sec for voltages slightly above the critcal voltage. As the pulse

voltage is increased, the delay time decreases to about $0.1\mu$ sec.

The next section describes the first generation of computer simulations of the delay-time switching process so that a comparison between the electrical behavior and thermally-based simulations may be made.

## III. Computer Simulations of Switching

Recent research reported at the most recent International Conference on Amorphous Semiconductors[2] revealed that the mechanisms of switching[3] are being somewhat clarified between thermal theories[4], "electrothermal" theories[5] and electronic theories[6]. These various investigations have each focused on particular amorphous semiconductors. The apparent confusion probably arises from the fact that switching occurs by different mechanisms in different materials and under different pulsing conditions (e.g. voltage, risetime of applied voltage, circuit resistance and inductance, etc.).

The current research in these laboratories focuses on switching in one amorphous semiconductor, AsTe, which has already received some study[1,7]. The experimentally observed switching characteristics are being compared with the computer simulations where the material's properties and circuit parameter used in the computer simulation match those used in the real case.

Consider a film of amorphous semiconductor, of thickness t, sandwiched between massive metal electrodes of diameter d. The length and width of the film is very large compared to the diameter of the electrodes and the thickness of the film. Orient a coordinate system such that the origin is at the center of the amorphous film on a line connecting the center of the electrodes and the x-y plane is oriented parallel to the semiconductor surface. If the conducting area, and thus the area heated in the sample, is considered to be

less than or equal to the area of the contacting electrodes then the heat transfer can be described by

$$\frac{d^2T}{dr^2} + \frac{1}{r}\frac{dT}{dr} + \frac{1}{r^2}\frac{d^2T}{d\varphi^2} + \frac{d^2T}{dz^2} + \frac{q'''}{k} = \frac{1}{\alpha}\frac{dT}{d\theta}$$ (1)

where   $\theta$ = time

$\varphi$ = angle from the x-axis

T = temperature

r = radial distance from the heat source

z = film thickness

k = thermal conductivity

c = heat capacity

w = specific weight

$\alpha$ = k/cw

The above configuration indicates that a hot element could be represented by a short finite cylinder whose length is t and radius r = ½d.  Schneider[8] and Carslaw and Jaeger[9] have shown that the temperature history at the geometric center of the cylinder, during cooling when no heat sources or sinks are present, is described by

$$\frac{T - T_a}{T_i - T_a} = P(\theta)\, C(\theta)$$ (2)

where   T = the temperature at any time $\theta$

$T_i$ = the uniform temperature of the element

$T_a$ = ambient temperature

and the functions P($\theta$) and C($\theta$) are given by

$$P(\theta) = \frac{4}{\pi}\left\{ \Sigma\frac{1}{n}\exp[(-\tfrac{1}{2}n\pi)^2\,\theta] \right\}$$ (3)

with $\Theta = \dfrac{4k}{cwt^2} \theta$ for all odd integers n $\hspace{3em}$ (4)

$$C(\Theta) = 2 \left\{ \sum_n [M_n J_n(M_n)]^{-1} \exp[(-M_n)^2 \Theta] \right\} \hspace{2em} (5)$$

with $\Theta = \dfrac{4k\theta}{cwd^2} = \dfrac{k}{cwr^2} \theta$ $\hspace{6em}$ (6)

Figure 1 shows the simulated (from equations (2) thrus (6)) cooling curves for a 2μm thin film contacted by electrodes of various radii. The progression from essentially radial heat transfer away from the filament axis to linear heat transfer perpendicular to the electrode surfaces is seen in the progression from an electrode radius of 1μm to a radius of 4μm. Radii larger than 4μm do not alter the temperature-time profile, indicating that for small thickness to radius ratios, $t/r \le 1/2$, cooling of a small filamentary volume is essentially represented by the cooling of an infinite plate.

Figure 2 represents cooling of a cylinder 2μm long with a 200μm radius from various uniform temperatures. It is seen that the region of thermal inertia varies from 0.6 microseconds at 350°K to 0.4 microseconds at 600°K. These results indicate that after reaching a particular temperature there is no significant cooling of the central portion of the filamentary area until after some finite period of time, approximately 0.5 microseconds for the system considered, has passed. Thus validating, at least in the initial stages of Joule heating, the assumption that there is no heat loss from the conducting volume. This is substantially shorter than the 5μ sec limit set by Fritzsche and Ovshinsky[10].

Most switching experiments utilize a circuit, similar to the one shown schematically in Figure 3, which has a current limiting resister $R_\ell$ in series with a semiconducting device, having a resistance $R_d$, and a voltage source.
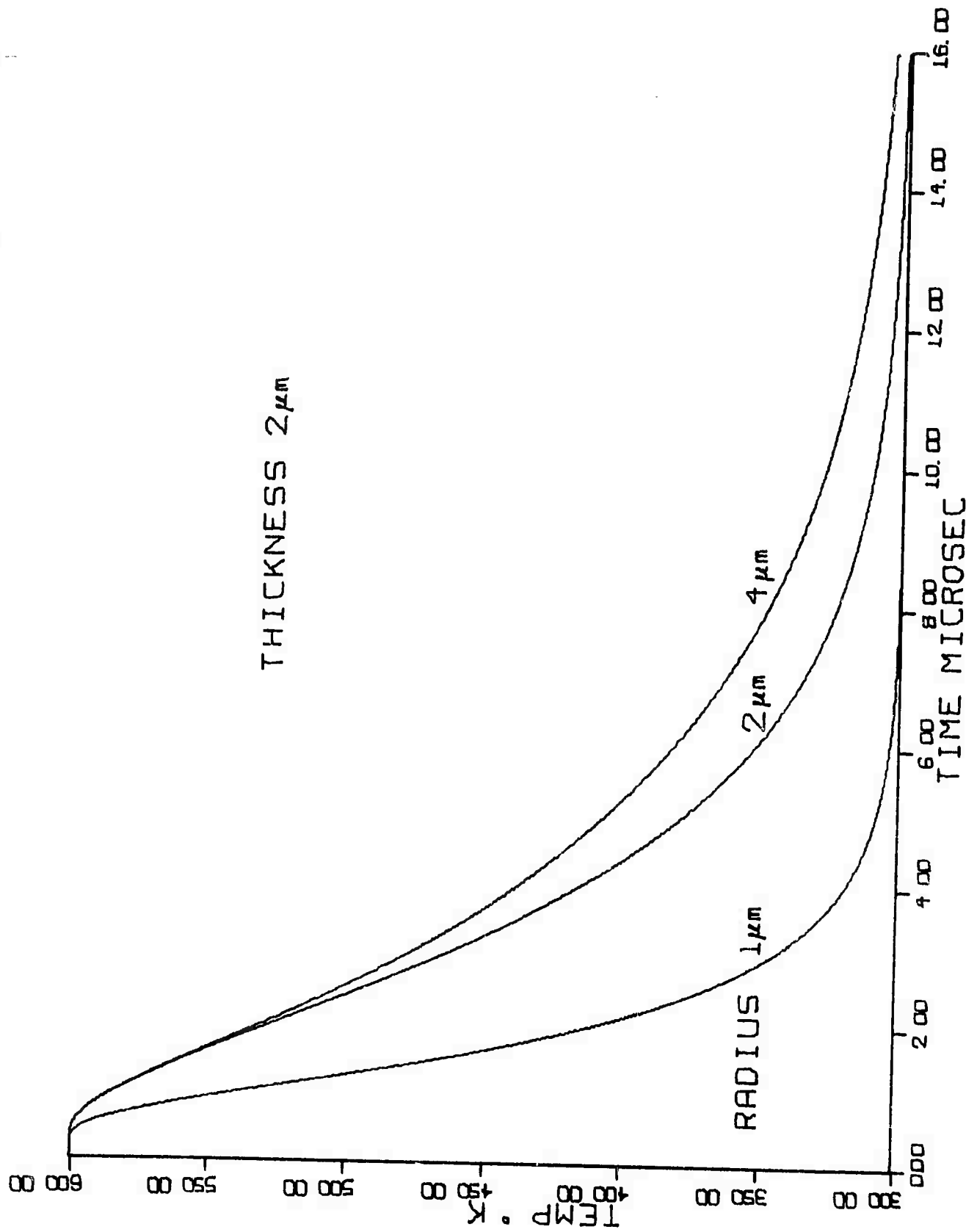
Figure 1. Simulated cooling curves for thin film filaments $2\mu m$ long with various electrode radii.

6

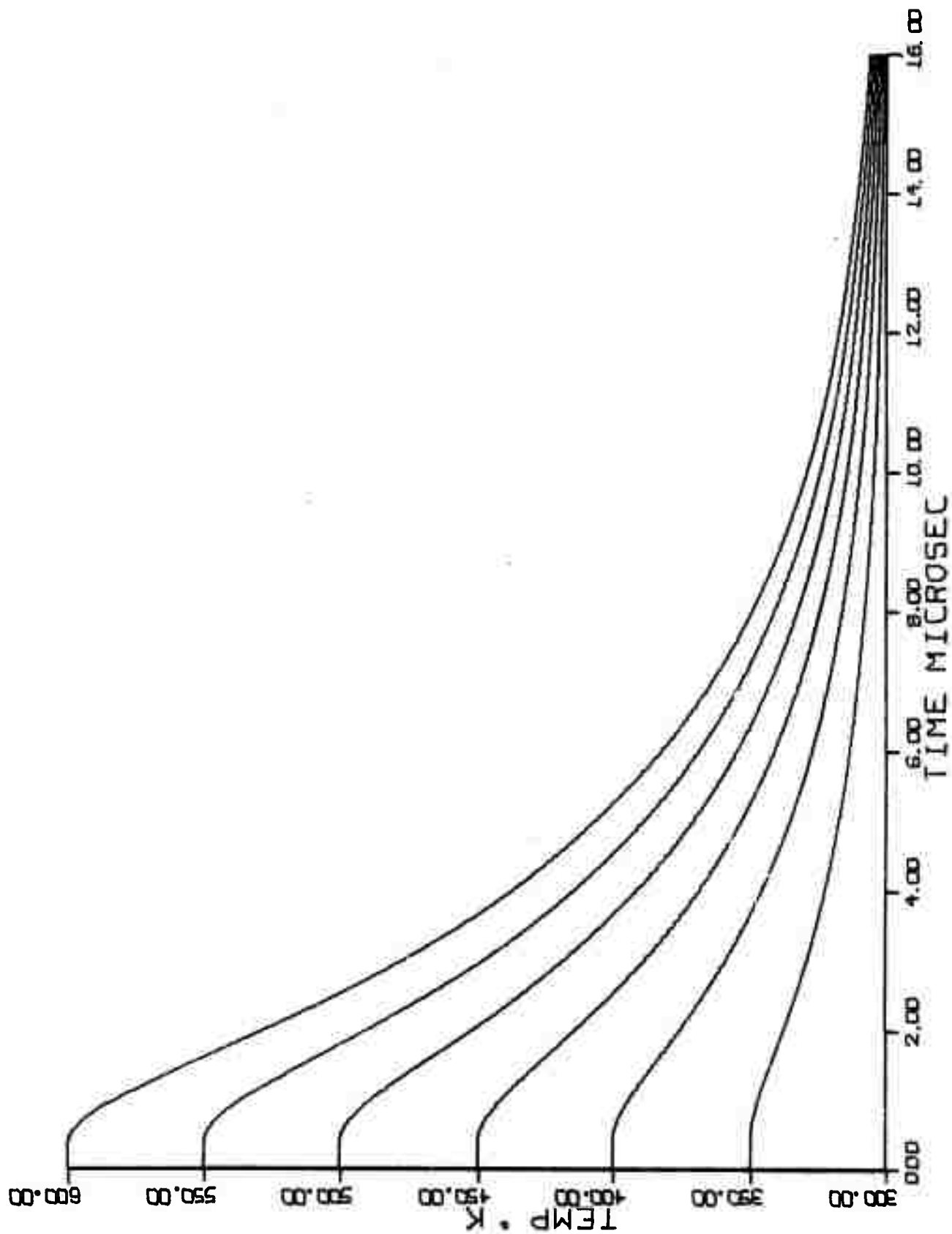Figure 2. Simulated cooling of a short finite cylinder 2μm in length and 200μm radius from various temperatures.

7

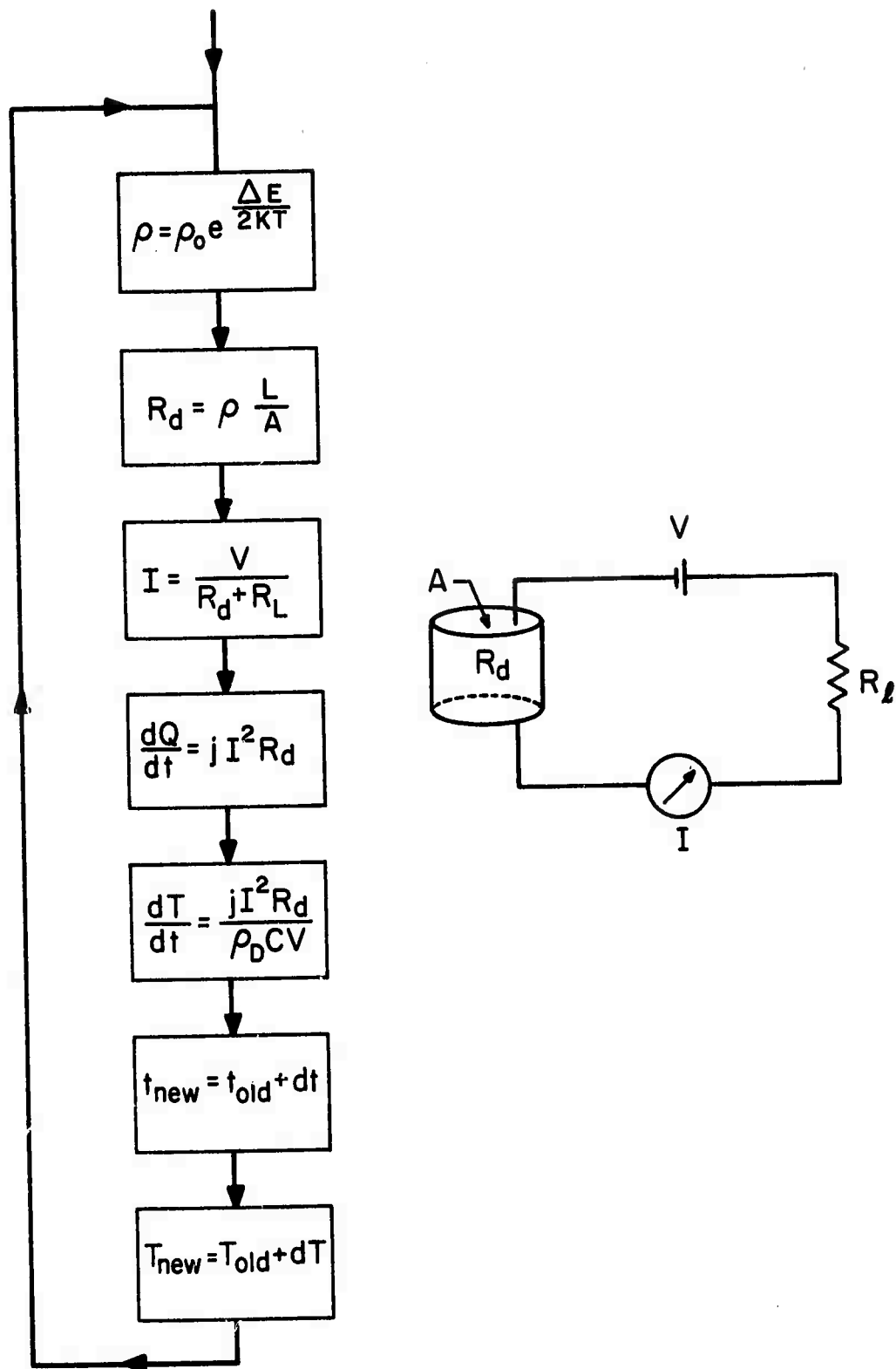Figure 3.   Schematic flow diagram of computer computations and schematic diagram of test circuit.

The voltage across the device, $V_d$, and the total current in the circuit are monitored simultaneously on oscilloscopes.

Representing the conducting area of the device as a wire of length, $t$, and cross-sectional area A. The heat per unit time generated in the wire is

$$\frac{dQ}{dt} = j\, I^2\, R_d \tag{7}$$

where $j$ = constant (0.239 cal/joule)

Considering the conducting volume to be isothermal its change in temperature with respect to time is given by

$$\frac{dT}{dt} = \frac{jI^2 R_d}{S_d CV} \tag{8}$$

where  I = current in amps

$S_d$ = density of semiconducting glass

$R_d$ = resistance of the device

C = heat capacity of the semiconducting glass

V = volume of semiconducting glass being heated

In equation (8) both current and device resistance are functions of temperature which must be expressed as functions of time for purposes of this simulation.

Referring to Figure 3, it is apparent that the following relation holds

$$I = V/(R_d + R_\ell) \tag{9}$$

It is known from experimental data that the voltage, V, supplied to the system remains constant, for a square wave pulse; hence, I varies inversely as $R_d$ since all other quantities are constant. Thus the analog reduces to generating $R_d$ as a function of time.

The resistivity of the glass used in switching devices can be described by a relation of the form

$$\rho = \rho_o \exp (E_o/T) \tag{10}$$

the slope of the resistivity-temperature relation at any temperature, prior to devitrification is

$$\frac{d\rho}{dT} = -\frac{E_o}{T^2} \rho \tag{11}$$

Equation (11) may be represented as a function of time by using the chain-rule

$$\frac{d\rho}{dT} = \frac{d\rho}{dT} \frac{dT}{dt} \tag{12}$$

substituting equations (8) and (11) into equation (12) yields

$$\frac{d\rho}{dt} = \left[-\frac{E_o}{T^2} \rho\right] \left[\frac{j\, I\, \rho\, L/A}{\rho_d\, CV}\right] \tag{13}$$

or

$$\frac{d\rho}{dt} = \left[-\frac{jE_o}{\rho_d CA^2}\right] \left[\frac{I\rho^2}{T^2}\right] \tag{14}$$

The digital simulation was accomplished using equations (8), (9), and (14). Time was used as the basic incrementing parameter beginning at room temperature (27°C) and continuing for various pulse lengths. The parameters, $\rho_o$, $E_o$, C, $P_D$, were determined in this laboratory[7].

The simulated data of Figure 4 and Table 1 indicate that as the radius of the filament increases the maximum temperature attained decreases. Considering the softening point of the glass of the simulated system, $T_s=355°C=628°K$[7], and tha the change in current with respect to time will be nearly zero at the temperature

Figure 4.

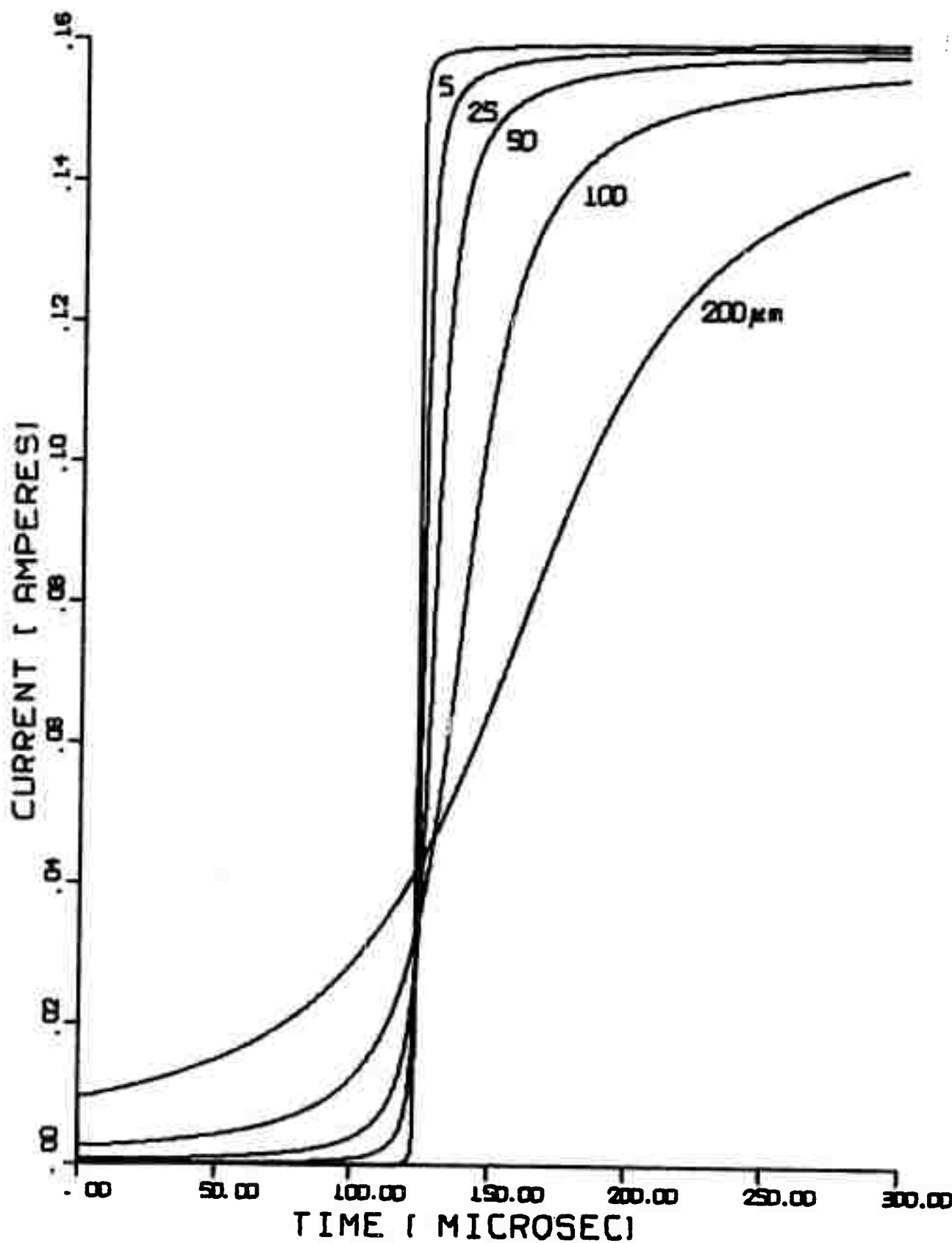SIMULATED SWITCHING OF 1μm THICK As-Te
FILM WITH VARIOUS FILAMENT RADII.

| RAD μm | Maximum Temp °K after 300μ sec | Total Heat Input Input Calories | Maximum Current |
|--------|-------------------------------|--------------------------------|-----------------|
| 5 | 4121 | $2.91 \times 10^{-7}$ | 159.67 |
| 25 | 980 | $1.29 \times 10^{-6}$ | 159.20 |
| 50 | 694 | $3.00 \times 10^{-6}$ | 158.16 |
| 100 | 525 | $6.88 \times 10^{-6}$ | 154.87 |
| 200 | 413 | $1.38 \times 10^{-5}$ | 142.10 |

Table 1.   Illustrating the interrelation among filament radius. maximum temperature, total heat input and maximum current level in various filaments 1μm in length.

maximum, then the radius of the filament should be approximately $100\mu m$. This corresponds to the radius of the contacting electrode used in the switching experiments[1]. The conclusion that the diameter of the conducting area during nonmemory switching is the same as for the contacts is further supported by photomicrographs presented in support of experimental data by Eusner, et al.[7], and Ultecht, et al.[11], which show a hot zone whose width corresponds to the diameter of the electrodes.

Figure 5 represents simulated switching at various applied voltages for a $1\mu m$ film using $200\mu m$ contacts. The delay time, $t_d$, for switching, at the previously defined point is well described by the empirical relation

$$t_d = A(1/V-V_o)^2 \tag{15}$$

where  A = constant

V = applied voltage

$V_o$ = the voltage at which an infinite amount of time would be required to cause switching.

This relation is in complete agreement with the experimental work reported by Sugi, et al.[12] For the system simulated A = 585.6 volts$^2$-sec and $V_o$ = 0.62 volts with $t_d$ in milliseconds.

Figure 6 is simulated switching using $200\mu m$ contacts on films of various thickness and a 16 volt potential. The delay time is seen to be a function of $\ell^2$ that can be expressed empirically by

$$t_d = 5.5 \times 10^{10} \ell^2 \tag{16}$$

with $t_d$ in milliseconds and $\ell$ in meters.

Taken together relations (15) and (16) indicate that the delay time for switching is expressed by a relation of the form
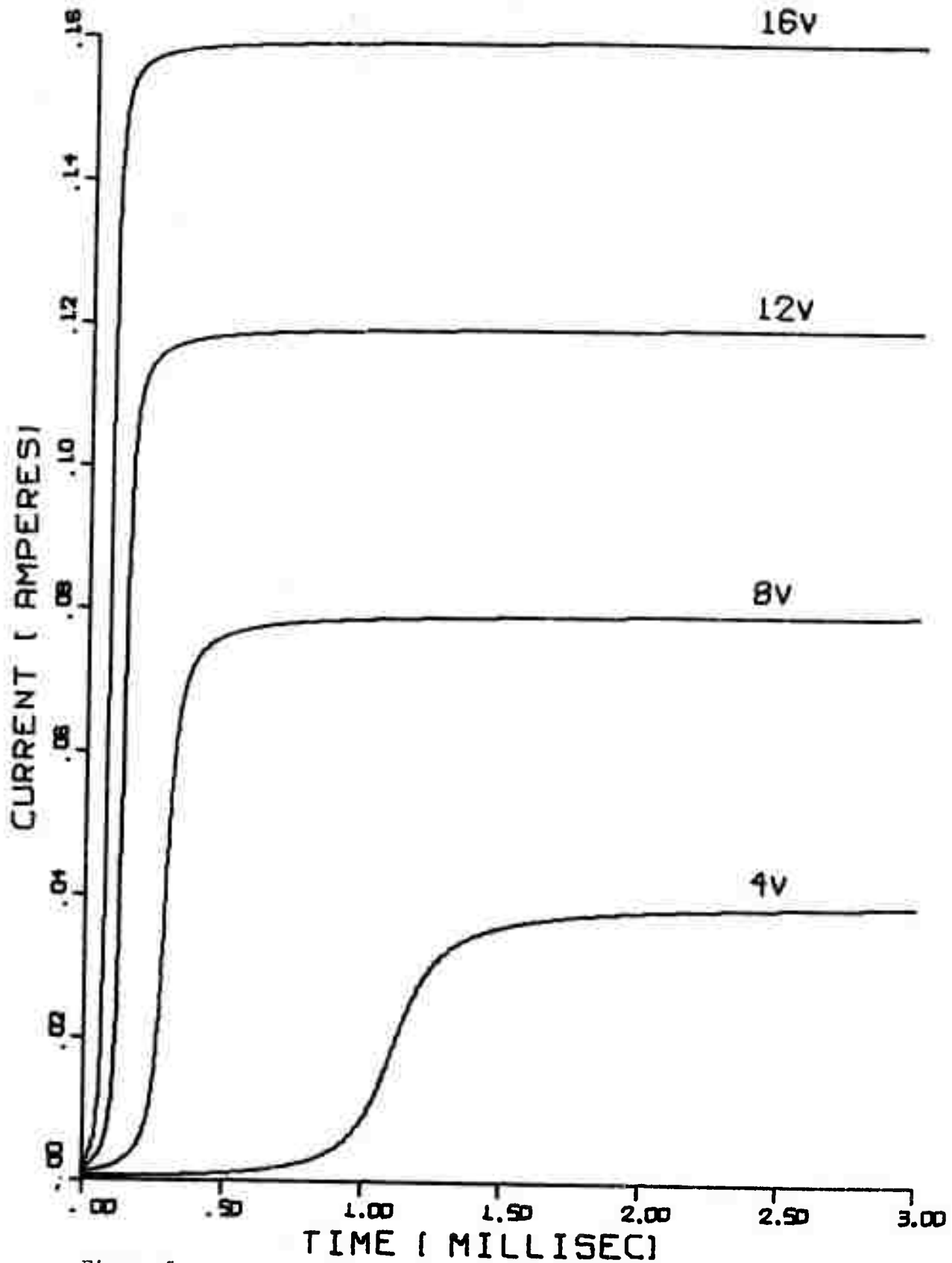
Figure 5.

SIMULATED SWITCHING OF 1μm THICK As-Te
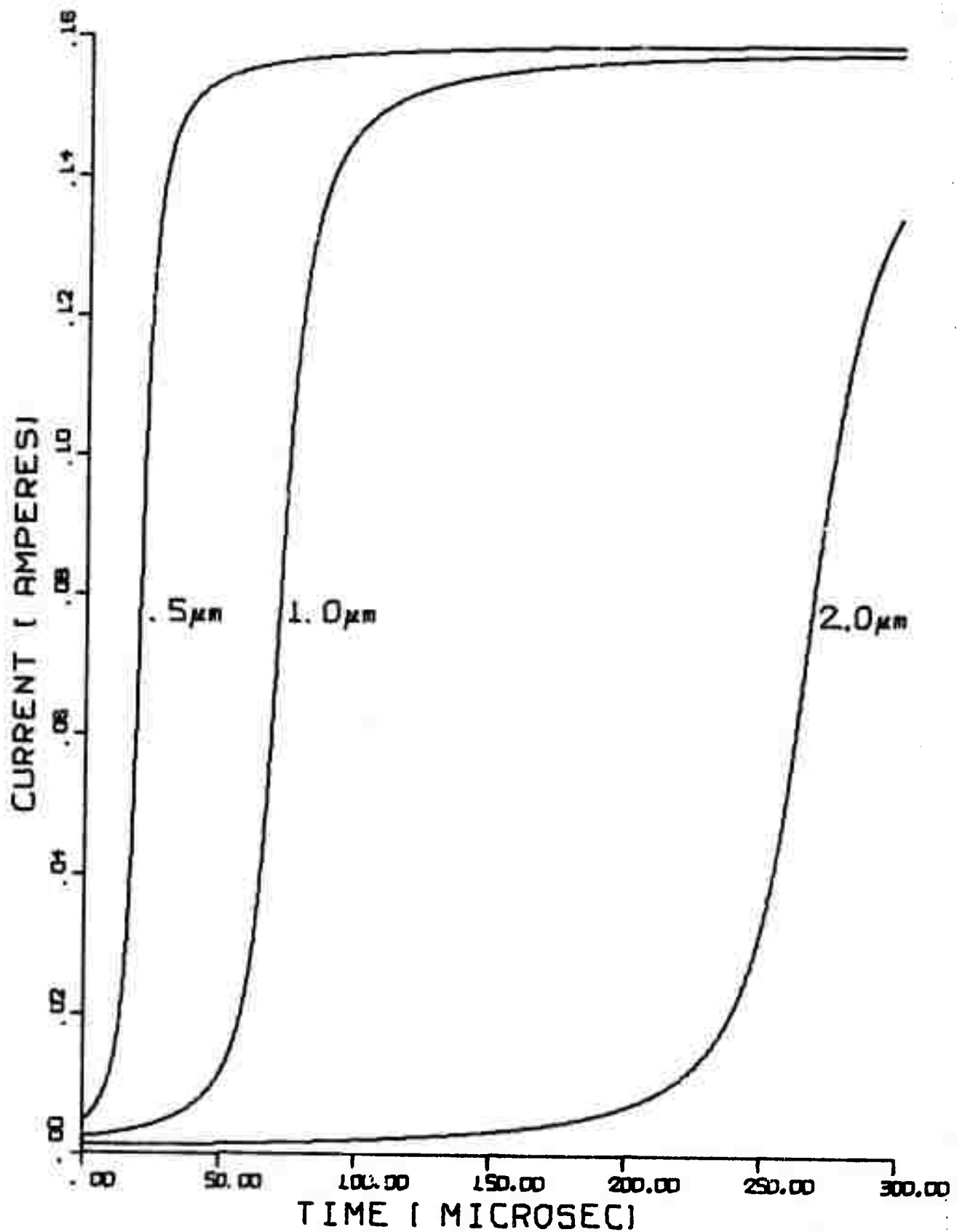FILM WITH 100μm FILAMENT RADIUS UNDER
DIFFERENT APPLIED VOLTAGES.

Figure 6.

SIMULATED SWITCHING OF 100μm RADIUS As-Te
FILAMENT VARYING FILM THICKNESS.

$$t_d \propto \left\{ \frac{\ell}{V-V_o} \right\}^2$$

(17)

This generally agrees with the results of other investigators[10,12], at least concerning the thickness dependence of delay time. The real difference is in the form of the expression for the voltage dependence, the delay time being inversely proportional to the square of the difference between the applied voltage and a reference voltage $V_o$.

Figure 7 shows the dependence of delay time on $\rho_o$. Shaw, et al.[1] indicate a minor switch at which time the conductivity increases by a factor of about five. This has been simulated by dividing $\rho_o$ by five. This results in a shifting of the temperature versus conductivity curve up by a constant amount.

Figure 8, like Figure 6, shows the effect of different thickness (i.e. from 0.1 to 0.5μm in 0.1μm steps) on switching characteristics. However, Figure 8a shows the same thicknesses, only a program has been added which now cools the filament after each increment. Inspection reveals the curves for 0.5μm on both Figures 8 and 8a are nearly identical leading to the conclusion that for a filament of thickness greater than or equal to 0.5μm cooling may be neglected.

In summary, the heat flow equation has been solved, digitally, for a real experimental system. The basic assumption is that there is no heat loss, from the conducting area, with respect to time. The resultant switching characteristics are shown to be similar to those of other investigators, any differences arising from the use of a square wave potential to induce switching and the simulation of a real test circuit.

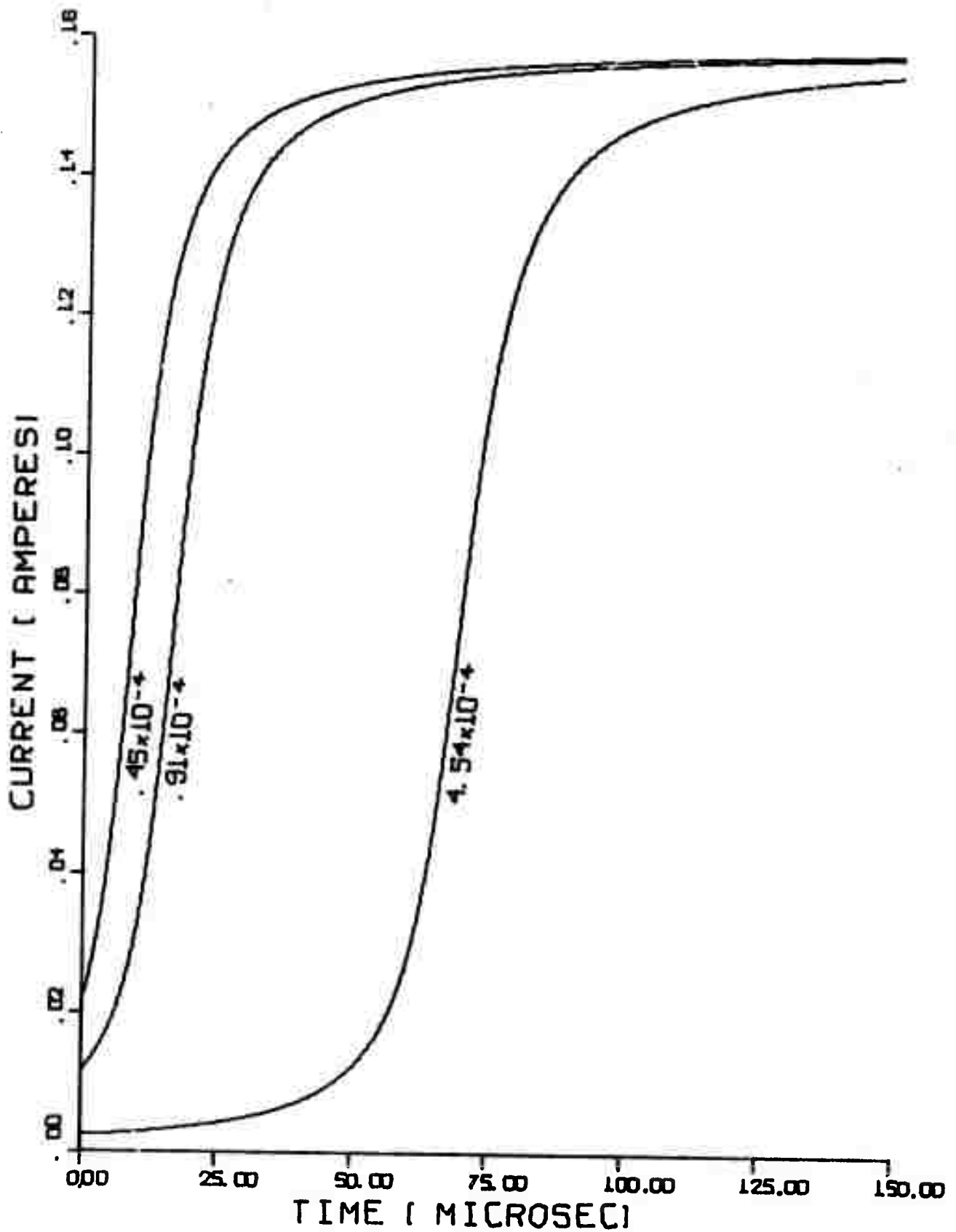It is shown that the delay time predicted from this simulation is directly

Figure 7.

SIMULATED SWITCHING OF 1μm THICK As-Te
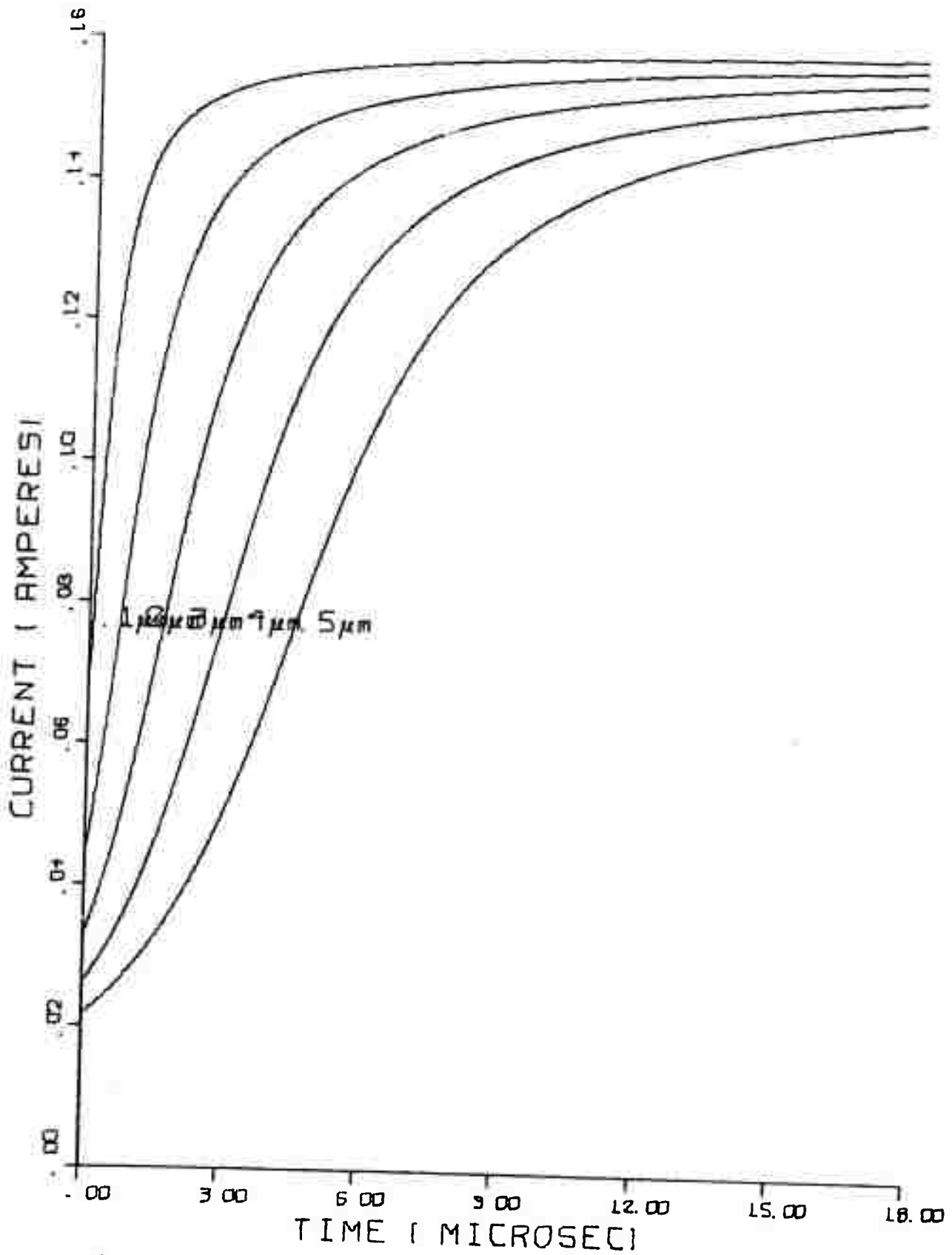FILM WITH 100μm FILAMENT RADIUS VARYING $\rho_0$.

Figure 8.

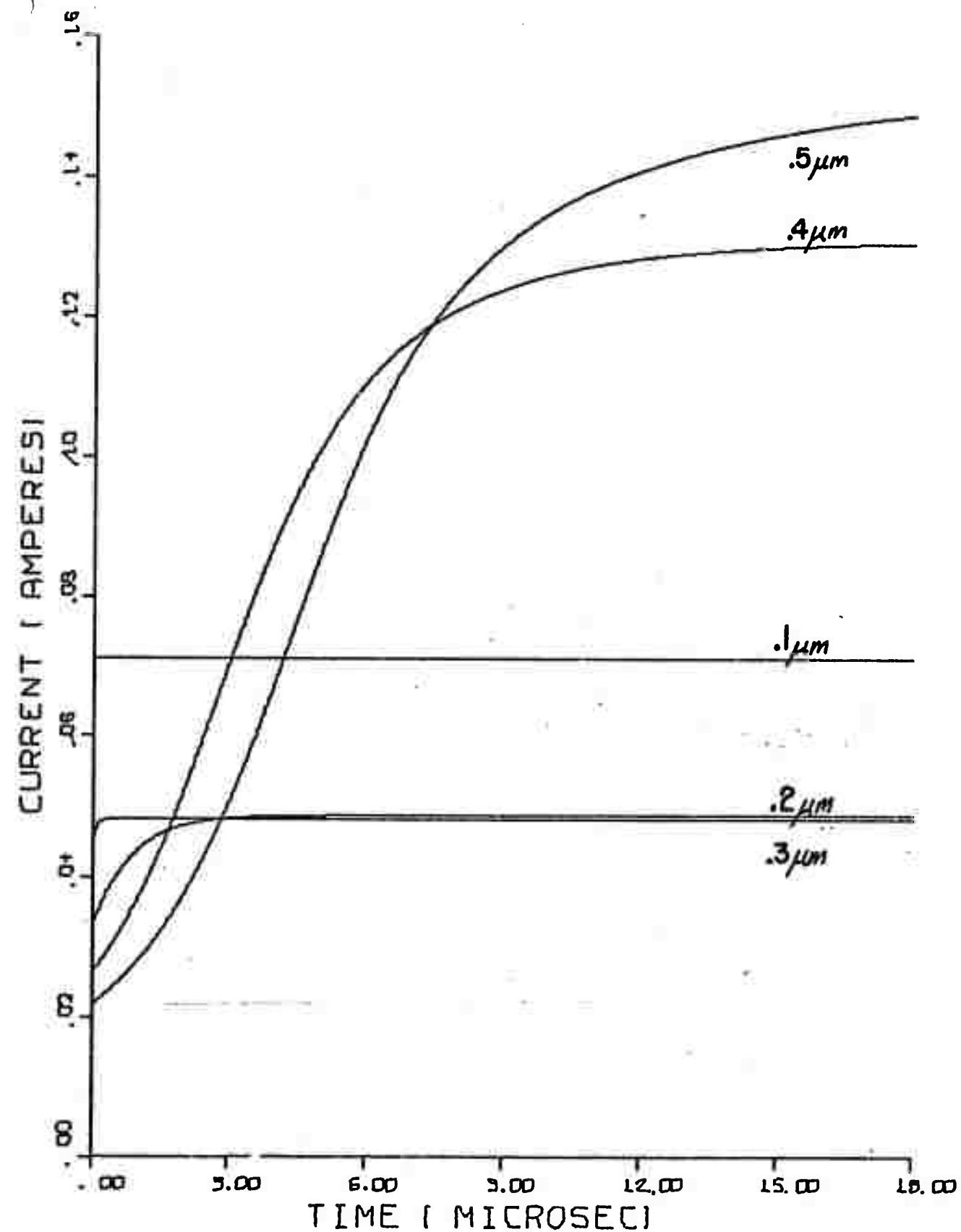SIMULATED SWITCHING OF 100μm RADIUS As-Te

FILAMENT VARYING FILM THICKNESS

Figure 8a.

SIMULATED SWITCHING OF 100μm RADIUS As-Te

FILAMENT VARYING FILM THICKNESS.

proportional to the square of the electrode separation and inversely prepor-
tional to the square of the difference between the applied potential and a
unique reference potential.

## IV. ESCA Studies

A portion of this study is devoted to utilizing ESCA (Electron Spec-
troscopy for Chemical Analysis) to develop a basic understanding of the
conduction mechanism in amorphous semiconductors.  Electron spectroscopy
should be well suited to a study of this kind since the data obtained is
directly proportional, in intensity, to the number of electrons occupying
a given energy level.  Before presenting a portion of the electron spectra
accumulated, it is useful to review the two conduction theories that are
most often used to describe electronic conduction in amorphous materials.

The polaronic hopping condition theory proposed by Mott[13,14,15,16]
is based on a spin diffusion model developed by Anderson[17] and extended
by Miller and Abrahams[18].  The essential elements of this theory are:

a.  The valance requirements of each atom are satisfied locally.

b.  There are extended states of localized energy levels above the
valance band and below the conduction band.  These states do
not overlap the fermi level and are separated by an energy gap
of the order $E_g \leq kT$.

c.  The activation energy for conduction is the energy of the band gap.
Conduction proceding by polaron assisted hopping from the extended
states of the valance band to extended states in the conduction band.

A second conduction model, proposed by Cohen-Fritzsche-Ovshinsky (CFO

model)[19], has the following distinctive features:

a. The localized states of the valance and conduction band tails actually overlap each other and the fermi level.

b. Localized conduction and valance band states are distinguishable as belonging to their respective bands even in the overlap region of the extended states.

c. There are well defined energys ev and ec in each band at which the transition from extended to localized states occurs.

d. The well defined activation energies reported for amorphous materials are the result of the activation of charge carriers from the fermi level to one of the localized states.

The two models of electronic conduction, presented above, are very similar in that they both postulate an electron diffusion mechanism, the main difference being due to visualization of the band gap. In the first model conduction occurs due to polaron assisted hopping between points of electrical discontinuity arising from defect type structues. Conduction in the second model results from extreme disorder in the material structure. However, in both cases the theoretical basis for a semi-quantitative description of the conduction phenomena is based on Anderson's theory and its extension by Miller and Abrahams.

Experimental evidence has been offered by several investigators[20,21,22,23] which seems to indicate that polaron assisted hopping is the primary mode of electronic conduction in solids containing multivalent components. Cohen[19] indicates that the CFO model is useful in explaining, at least qualitatively, optical absorption, photoconductivity, electronic field effects, ohmic contacts, recombination radiation, and radiation hardness effects.

ESCA is well suited to studying the energy levels actually occupied by

electrons and has been rather extensively used in studies of chemical bonding. Since the development of the high resolution electron spectrograph by Sieghahn and his coworkers in 1968, many organic compounds have been studied to ascertain the different bonding arrangements of a single atom in a complex molecule. The band structure of some metallic compounds have been studied by Novakov[24], Hamrin[25], and Ramquist[26]. It is clear that any ESCA study whose aim is to develop an understanding of the conduction mechanism must be conducted in two parts:

i. A study of outer valence electron levels.

ii. A study of the ionic species present as determined from the strongest exitation level of each atomic species.

To this end the system As-Te was selected for study, partially due to familiarity with the system and partially because it is a simple system representative of the chalcogenide glasses that are semiconducting and exhibit both bistable and memory switching phenomena.

ESCA samples of amorphous $AsTe_{1.07}$, crystalline $AsTe_{1.07}$, and stochimetric $As_2Te_3$ were prepared by grinding to a fine powder under ethyl alcohol in a dry box flushed with forming gas, then cold pressing into a 48 mesh copper screen to 20,000 psi. Electron spectra were collected over 80 ev of binding energy beginning at 78 ev and decreasing in 0.2 ev steps. The results are shown in Figures 9 and 10. The binding energies shown represent the true binding energies in the solids being investigated. The only notable difference between Figure 9 and 10 is the beginning of an oxide peak, labeled $\varphi$, in Figure 10. The obvious conclusion being that there is little difference in the structure of the glass and the crystalline material. Further confirmation of this conclusion was gained by examining the 3d electron levels of tellurium metal, $TeO_2$, amorphous $AsTe_{1.07}$, crystalline $AsTe_{1.07}$, and stochiometric $As_2Te_3$.
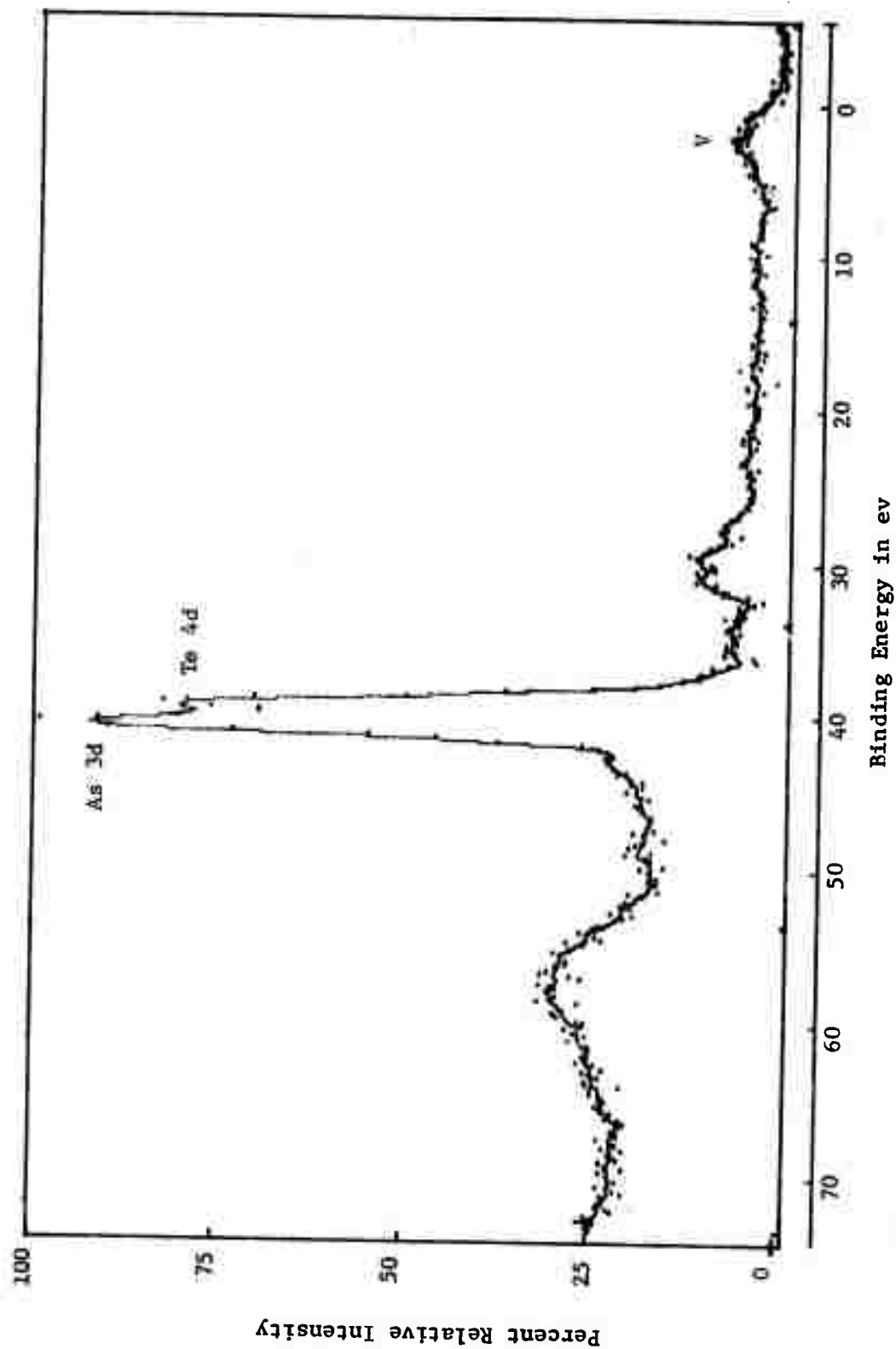
Figure 9. Eighty ev scan of amorphous AsTe$_{1.07}$ covering the outer energy levels.

22
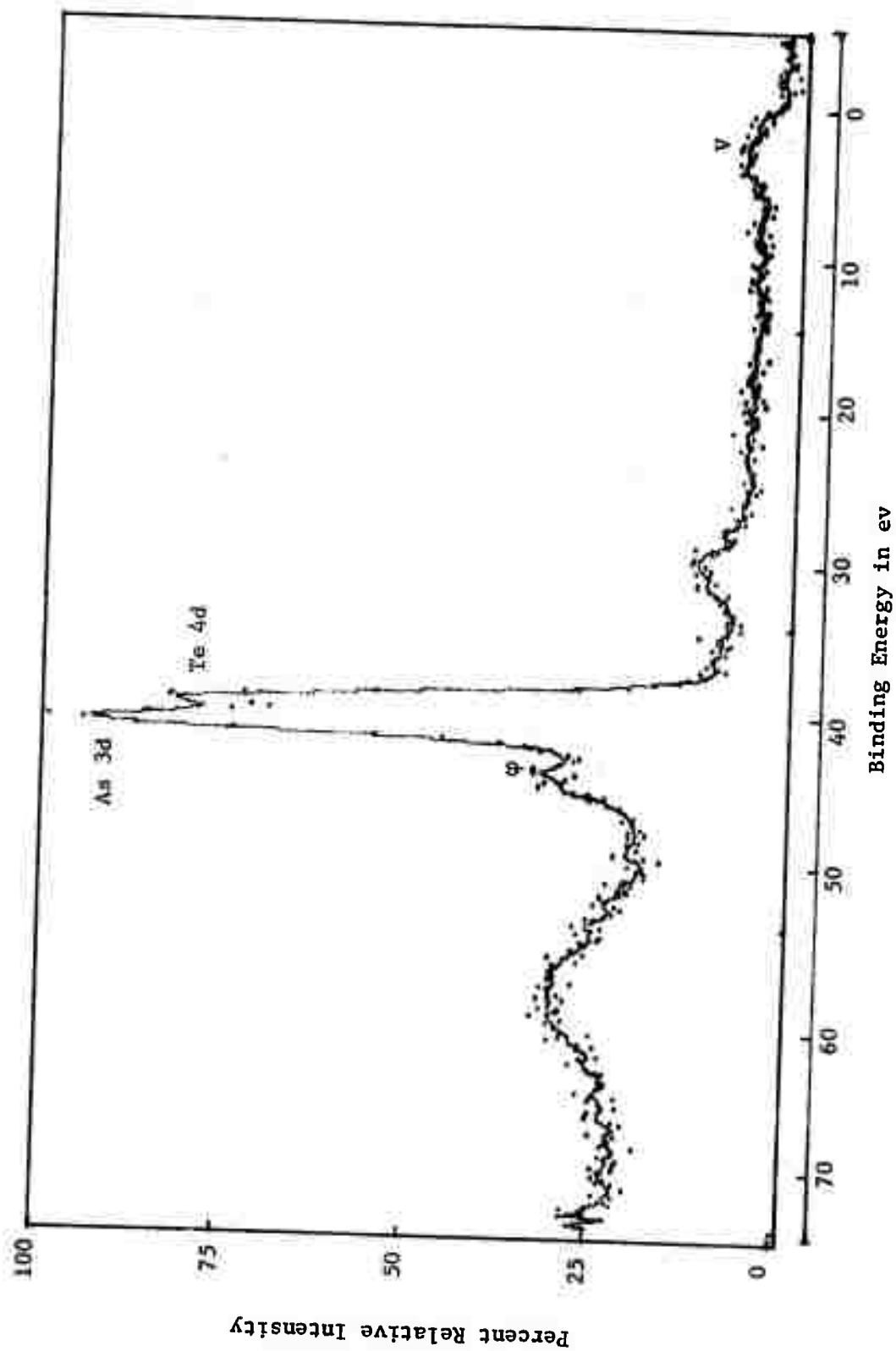
Figure 10. Eighty ev scan of crystalline AsTe$_{1.07}$ covering the outer energy levels.

23

Twenty ev scans for each of these materials are shown in Figures 3 thru 7.
Each scan begins at 589 ev of binding energy and ends at 569 ev of binding
energy.

The binding energy shift for the 3d electrons of tellurium, from the
pure state to the oxide, is seen from Figures 11 and 12 to be an increase
of 3.4 ev of binding energy.

There is no evidence of peak shift or broadening when Figures 13, 14,
and 15 are compared to Figure 11 indicating that there is little or no
ionic charter in As-Te bands.  This is as would be expected since Pauling's
electronegativities indicate that there would be 0.5% ionic character for
As-Te bonds compared to 39% ionic character for Te-O bands.

Examination of binding energies in the range 50 ev - 30 ev shown in
Figures 16 thru 18, which includes the arsenic 3d electrons and the tellurium
4d electrons, also indicates that there is little difference among the elec-
tronic structures of the amorphous, crystalline, and stochiometric samples.
This suggests that the hopping mechanism may not be valid for these materials.
However, such a conclusion would require more data and it must be remembered
that only those electron states that are occupied by a large enough number
of electrons so that the probability of detection is significant are recorded
by ESCA.

Clearly, more spectural studies are needed to clarify the conduction mech-
ism, particularly studies of the outer electron levels near the zero of binding
energy.  As seen in Figure 9 and 10, labeled V, these are low intensity peaks
and on the scale at which these studies were conducted appear to be identical.
However, the differences in electrical conductivity between the amorphous and
crystalline materials, $10^{-4}$ and $10^{-2}$ mhos/cm at $25^{o}$C, indicate that there
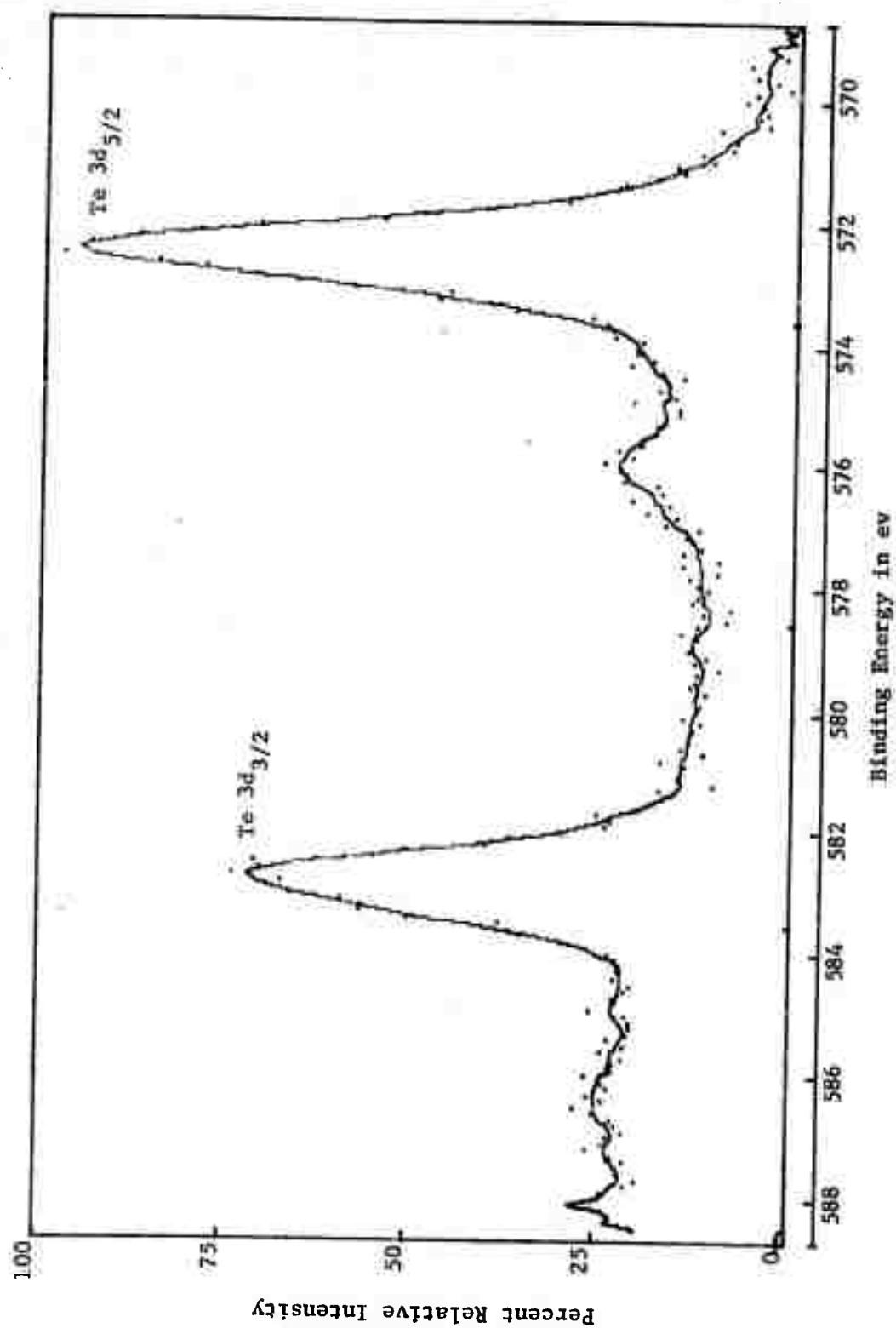should be some difference.

Figure 11. Three d electron levels of a tellurium metal standard.
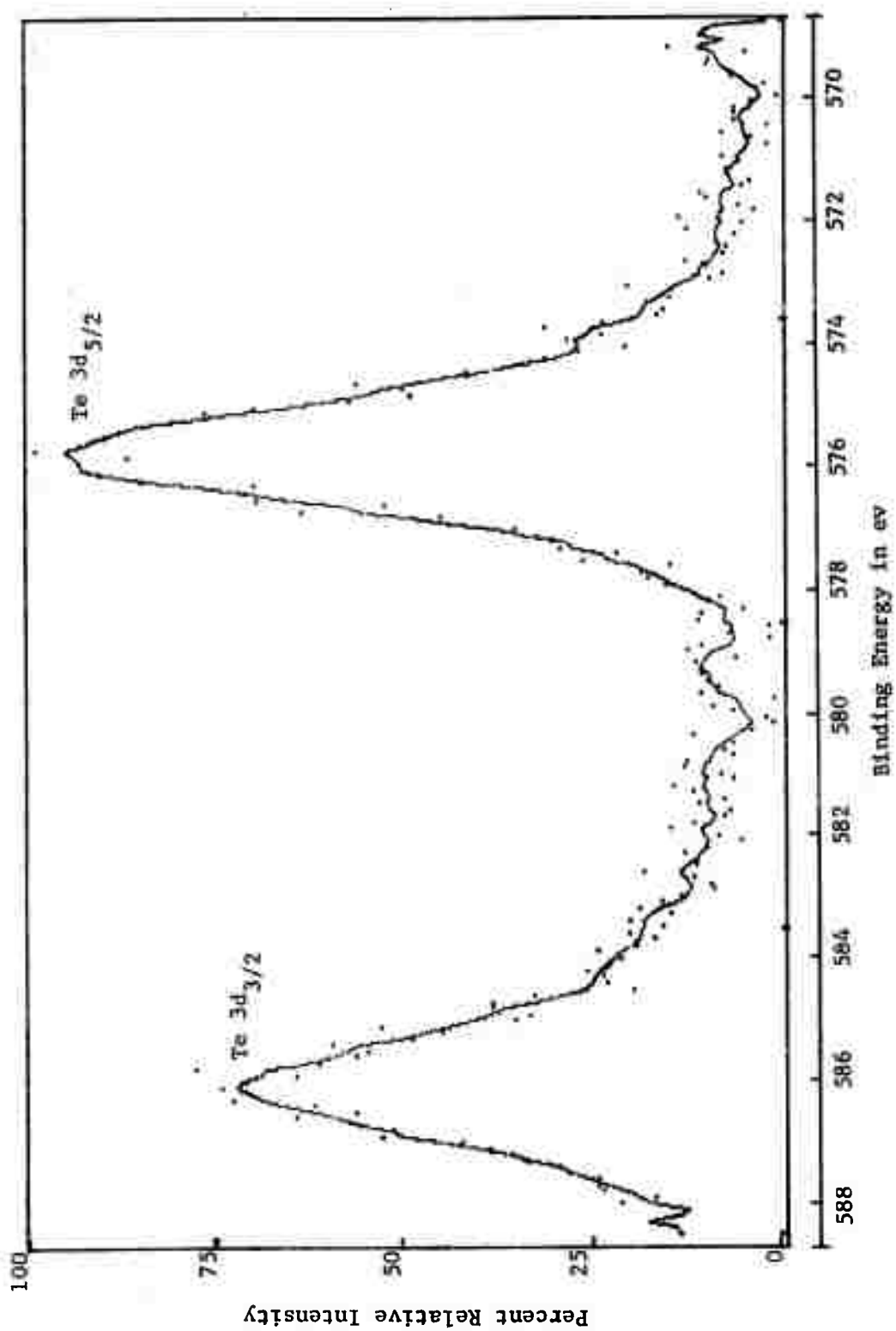
25

Figure 12. Tellurium 3d levels from TeO₂.

26
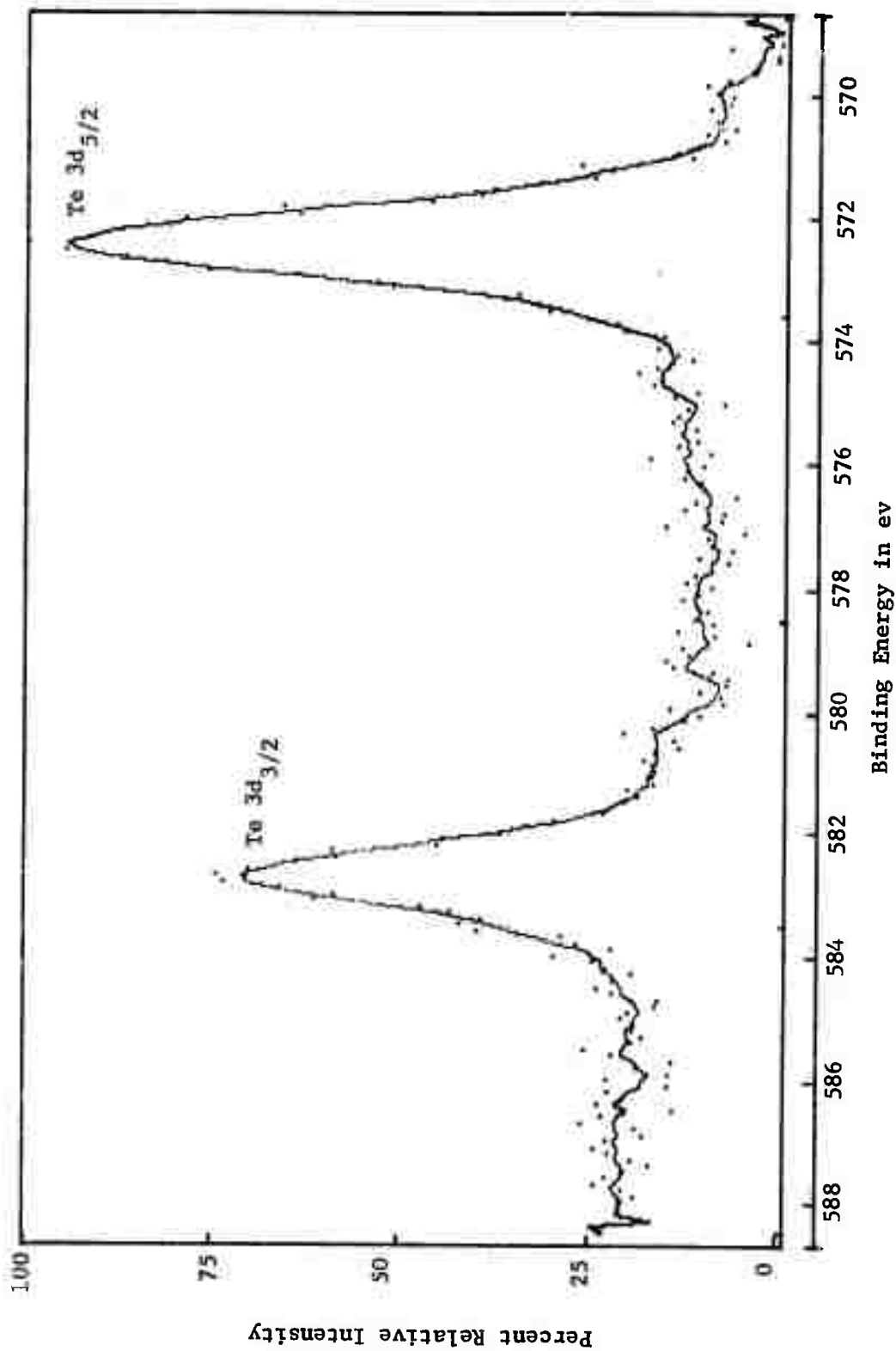
Figure 13. Tellurium 3d levels of crystalline AsTe$_{1.07}$.

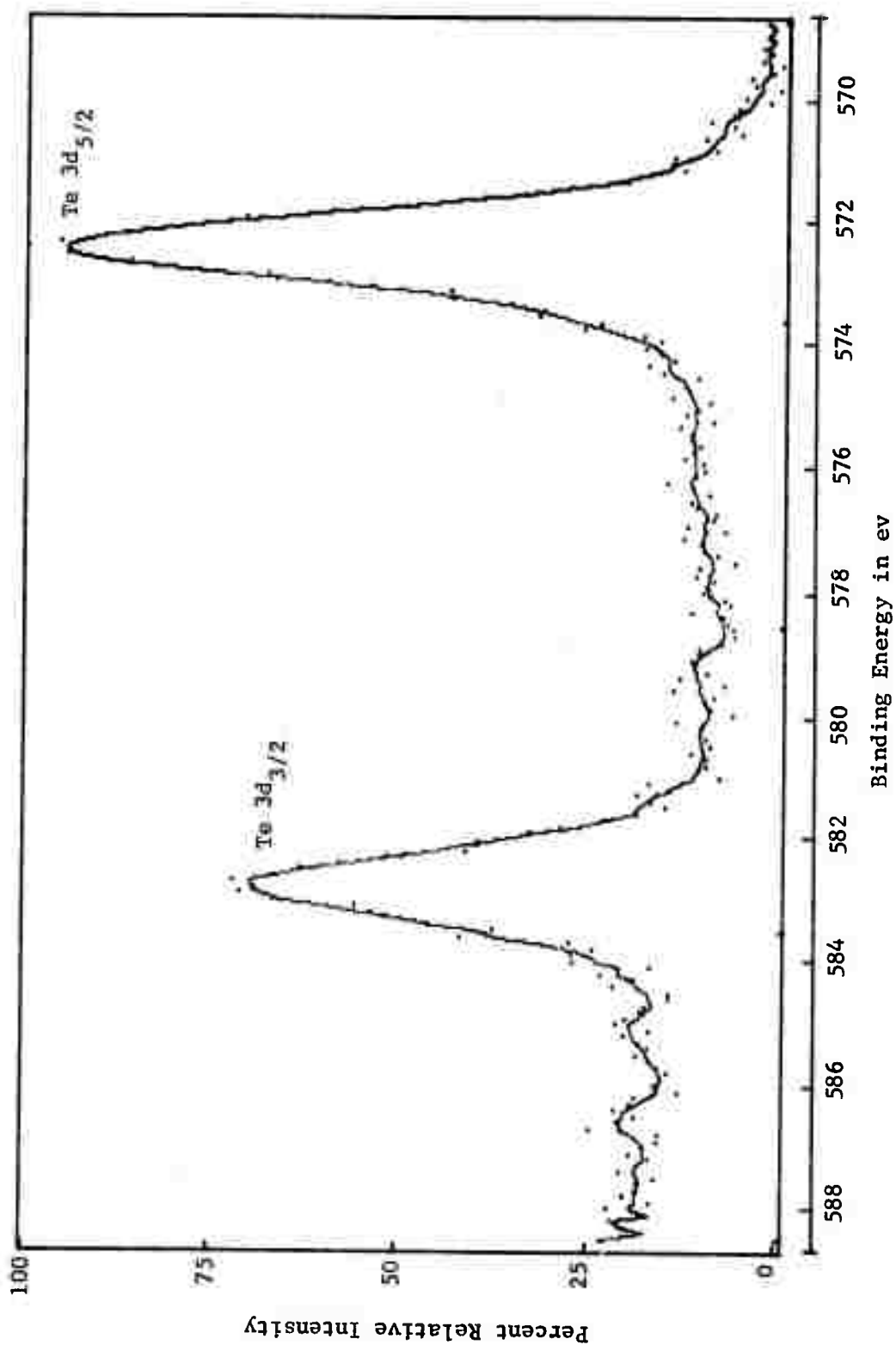Figure 14. Tellurium 3d doublet from amorphous AsTe$_{1.07}$.

28

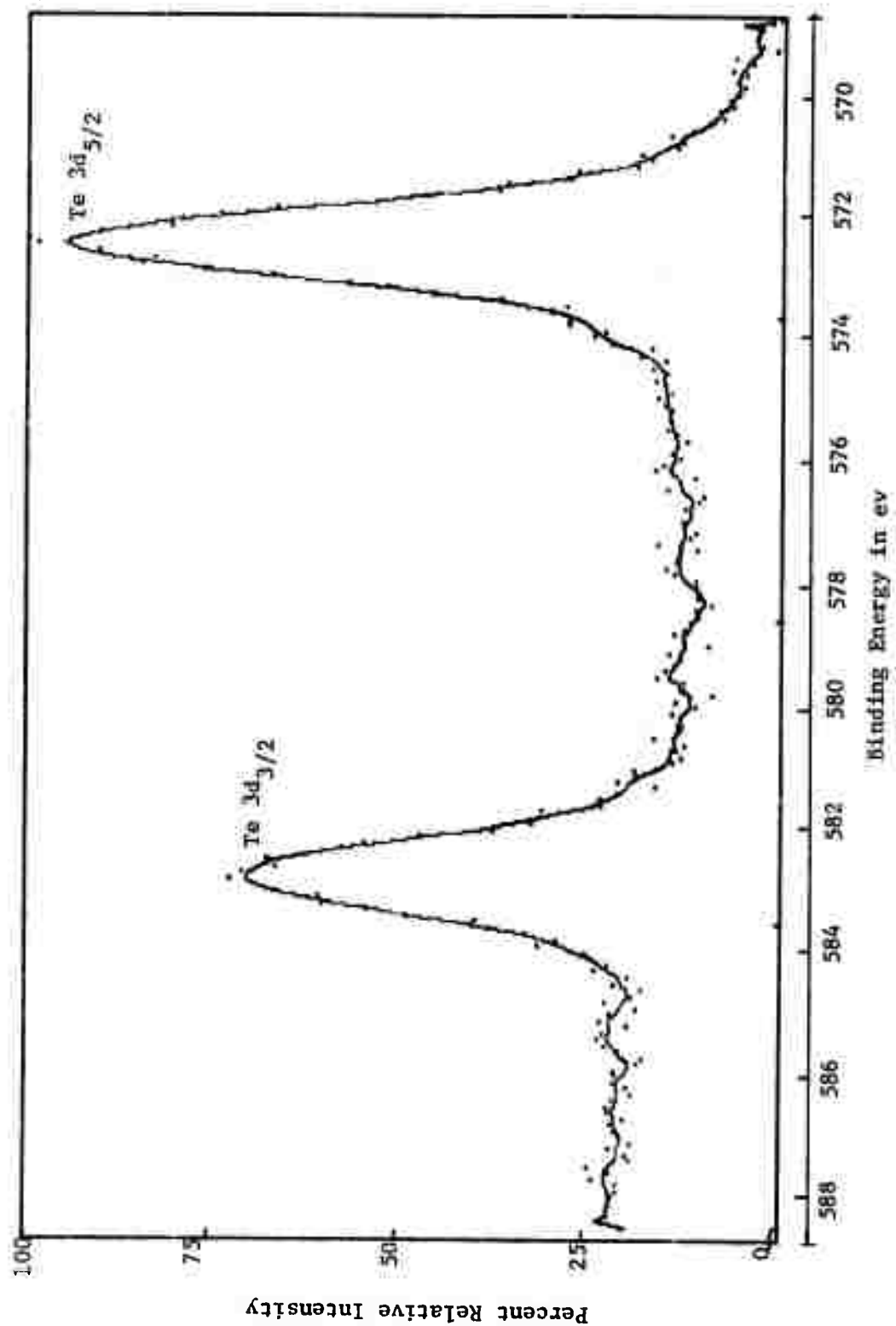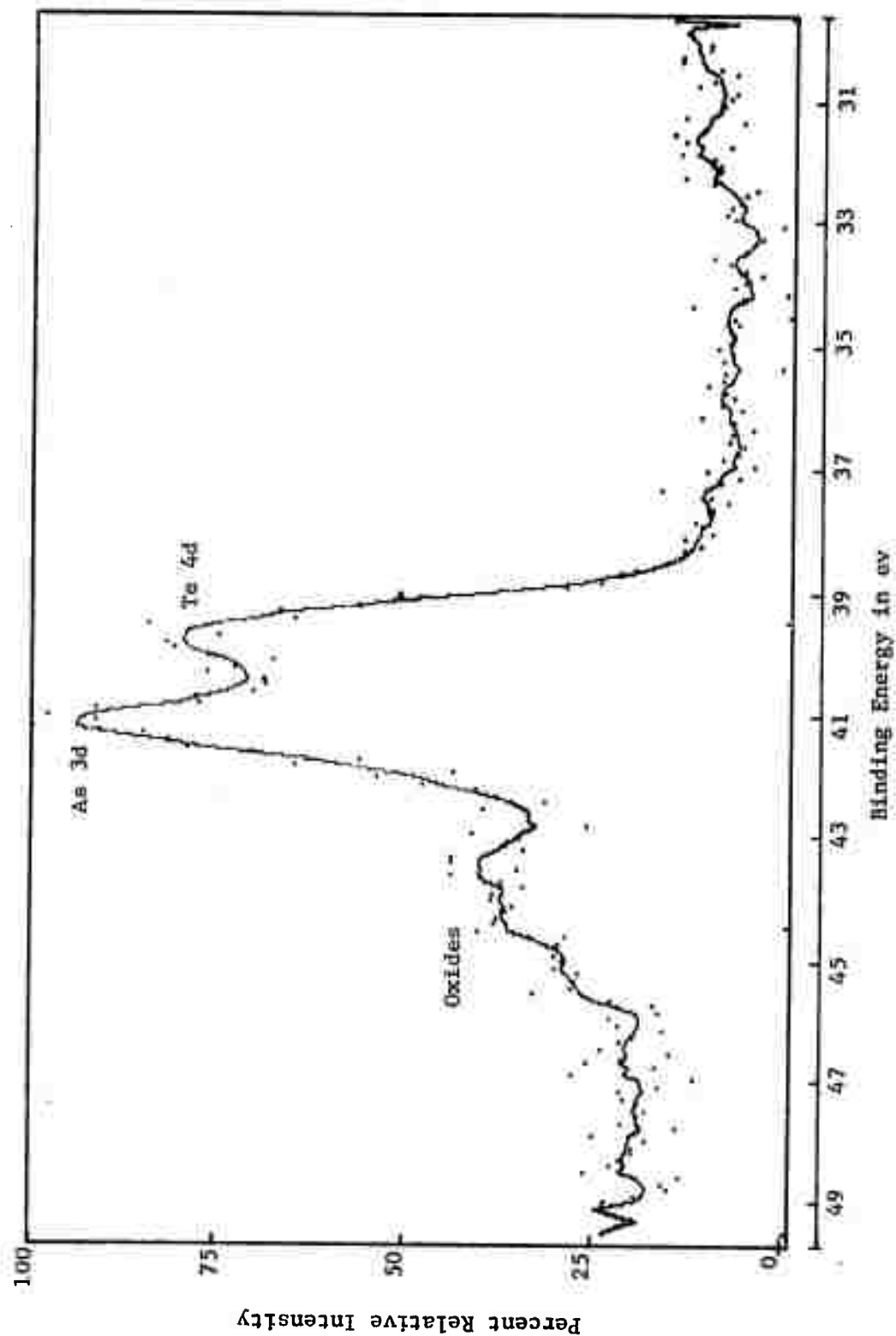Figure 15. Tellurium 3d doublet from stochiometric $As_2Te_3$.

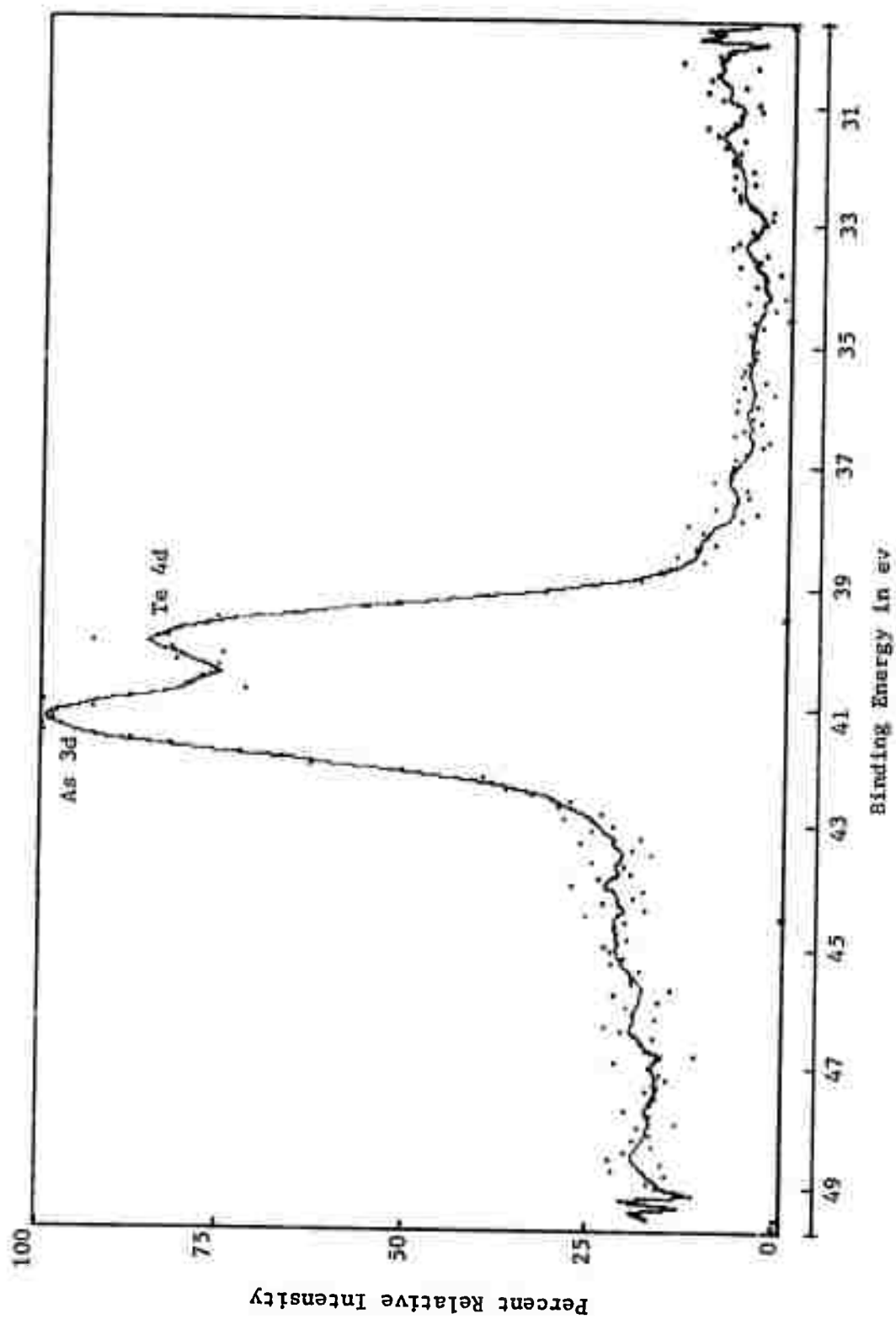Figure 16. Arsenic and tellurium, 3d and 4d electron levels from crystalline AsTe$_{1.07}$.

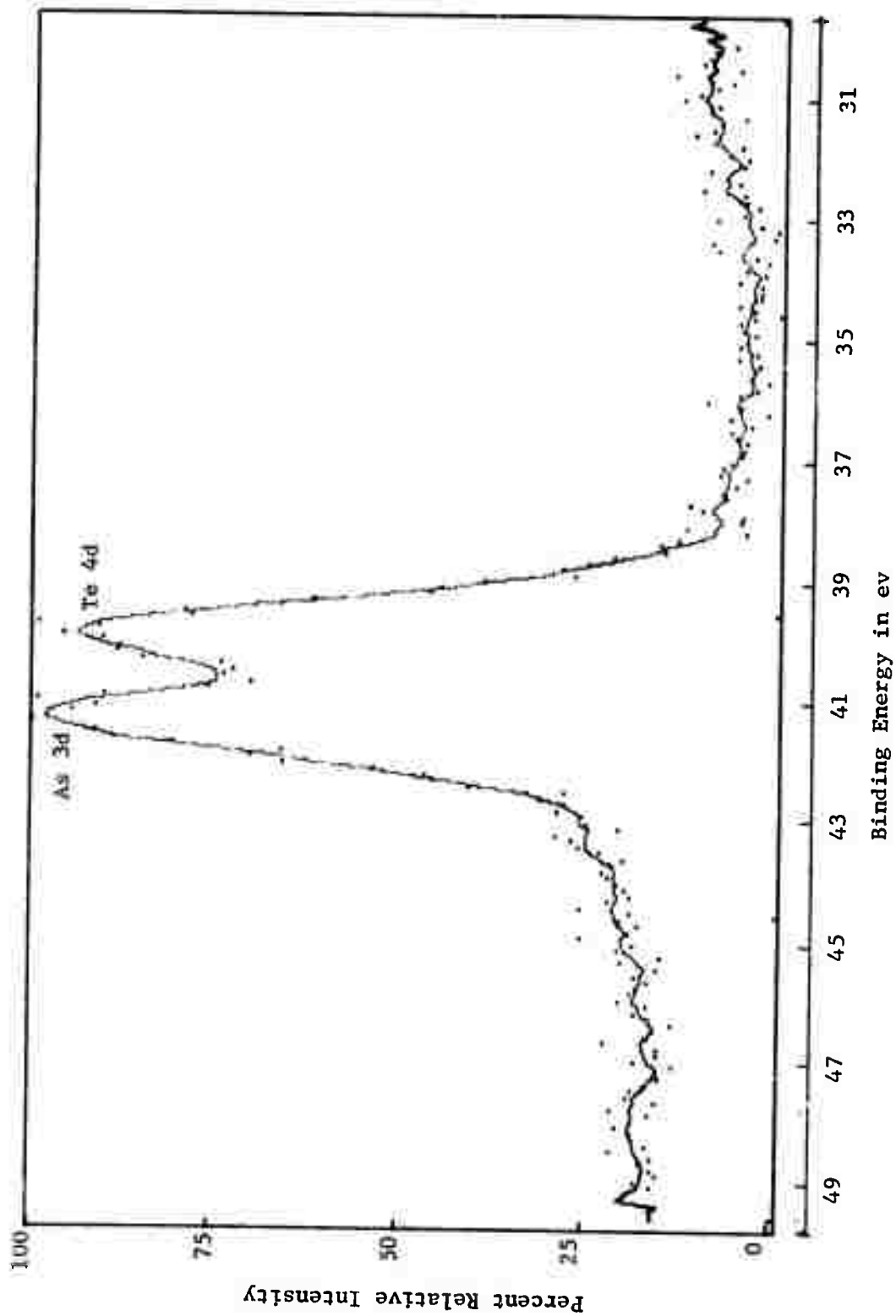Figure 17. Arsenic and tellurium, 3d and 4d electron levels in amorphous AsTe$_{1.07}$.

31

Figure 18. Arsenic and tellurium, 3d and 4d electron levels in stochiometric $As_2Te_3$.

## V. Future Work

The experimental studies of switching, started prior to this project, were performed on samples in which the geometry of the active amorphous semiconductor could not be determined with great accuracy because the top electrode was a metallic hemisphere pressed against the amorphous semiconductor film. Current research includes the fabrication of thin film arrays in which all geometries are accurately known. Although past work has focused on a familiar amorphous semiconductor (AsTe), future work will include other materials. It is believed that a more conducting amorphous semiconductor will demonstrate delay-time switching at voltages lower than those needed for the minor switch. If this is true, a regime of resistivities can be defined in which switching is strictly thermal. The determination of the physical parameters (electrical and thermal conductivity, heat capacity, and density) is continuing.

The minor switching phenomenon observed in AsTe is the focus of new research. In particular, the effect of the circuit properties (inductance, capacitance, resistance) on the minor switching characteristics will be determined to gain an improved understanding of this phenomenon.

A continuous effort is being made to eliminate all assumption in the simulation of thermal switching. For example, heat loss from the active region is known to be important for low voltage, long delay time, switching. Future simulations of the current rise will correct for the heat transfer during the heat-up process.

The ESCA studies will focus on the shape of the occupied valence electron bands in an effort to understand the difference between the electrical properties of amorphous and crystalline semiconductors of the same

composition. Care is now being taken to obtain only the electronic spectrum of the amorphous semiconductor without that from the sample holder. All future samples for ESCA and for the electrical experiments will be radio frequency sputtered thin films.

Written by:

W. D. Leahy, Jr.
Graduate Research Assistant

L. R. Durden
Research Instructor

L. H. Slack
Principal Investigator

## References

1. Shaw, M. P., Moss, S. C., Kostylev, S. A., and Slack, L. H., "Pre-switching and Post-Switching Phenomena in Amorphous Semiconducting Films," unpublished, attached.

2. Proc. Fourth Int. Conf. Amorph. and Liq. Semiconductors (Aug. 1971), J. Non-Cryst. Solids, 8-10 (1972), in press.

3. For general discussions of switching, see:
   (a) D. Adler, Critical Reviews in Solid State Sciences, 2, 317 (Chem. Rubber Pub. Co., Cleveland, Ohio, 1971).
   — (b) C. N. Bergland and N. Klein, Proc. IEEE, 59, 1099 (1971).

4. For recent reports favoring a thermal mechanism for switching, see:
   (a) H. J. Stocker, J. Appl. Phys. Lett., 15, 55 (1969).
   (b) A. D. Pearson and C. E. Miller, Appl. Phys. Lett., 14, 280 (1969).
   (c) D. F. Weirauch, Appl. Phys. Lett., 16, 72 (1970).
   (d) I. Balberg, Appl. Phys. Lett., 16, 72 (1970).
   (e) P. Jochen, Electronics Lett., 6, 461 (1970).
   (f) P. Burton and R. W. Brander, Int. J. Electronics, 27, 517 (1969).
   (g) W. W. Sheng and C. R. Westgate, Solid State Comm., 9, 387 (1971).
   (h) R. Hostrom, Roc. IEEE, 57, 1451 (1969).
   (i) E. L. Cook, J. Appl. Phys., 41, 551 (1970).

5. Kaplan, T., and Adler, D., Appl. Phys. Lett., 19, 418 (1971).

6. van Roosbroeck, W. and Casey, Jr., H. C., Phys. Rev., 5B, 2154 (1972); and van Roosbroeck, W., Phys. Rev. Lett., 28, 1120 (.972).

7. Eusner, P. R., Durden, L. R., and Slack, L. H., "Unusual Electrical Effects in As-Te, Semiconducting Glasses," J. Amer. Ceram. Soc., 55, 1, 43-46 (1972).

8. Schneider, P. J., Conduction Heat Transfer, Addison-Wesley Publishing Co., (1957).

9. Carslaw, H. S., and Jaeger, J. C., Conduction of Heat in Solids, Oxford University Press, (1959).

10. Fritzsche, H. and Ovshinsky, S. R., "Conduction and Switching Phenomena in Covalent Alloy Semiconductors," J. Non. Cryst. Solids, 4, 464-479 (1970).

11. Ultecht, R., Stevenson, H., Sie, C. H., Griener, J. D., and Raghaven, K. S., "Electric Field-Induced Filament Formation in As-Te-Ge Glass," J. Non. Cryst. Solids, 2, 358-370 (1970).

12. Sugi, M., Kikuchi, M., and Iizima, S., "Switching Characteristics of Chalcogenide Glass," Solid State Communications, 1, 1805-1807, (1969).

13. Mott, N. F., "Conduction in Glasses Containing Transition Metal Ions," J. Non. Cryst. Solids, 1, 1-17, (1968).

14. Mott, N. F., "Conduction in Non-Crystalline Systems I. Localized Electronic States in Disordered Systems," Phil. Mag., 17, 1259-1268, (1968).

15. Mott, N. F., and Davis, E. A., "Conduction in Non-Crystalline Systems II. The Metal-Insulator Transition in a Random Array of Centers," Phil. Mag., 17, 1269-1284, (1968).

16. Mott, N. F., "Conduction in Non-Crystalline Materials III. Localized States in a Pseudogap and Near Extremities of Conduction and Valence Bands," Phil. Mag., 19, 835-852, (1969).

17. Anderson, P. W., "Absence of Diffusion in Certain Random Lattices," Physical Review, 109, 5, 1492-1505,(1958).

18. Miller, Allen, and Abrahams, Elihu, "Impurity Conduction at Low Concentrations," Physical Review, 120, 3, 745-755, (1960).

19. Cohen, M. H., "Electronic Structure and Transport in Covalent Amorphous Semiconducting Alloys," J. Non. Cryst. Solids, 2, 432-443, (1970).

20. Clark, A. H., "Electrical and Optical Properties of Amorphous Germanium," Physical Review, 154, 750-757, (1967).

21. Walley, P. A., and Jonscher, "Electrical Conduction in Amorphous Germanium," Thin Solid Films, 1, 367-377, (1968).

22. Spring-Thorpe, A. J., Austin, I. G., nd B. A., "Hopping Conduction in $Li_xNi_{1-x}O$ Crystals at Low Temperatures," Solid State Communications, 3, 143-146, (1965).

23. Sayer, M., Mansingh, A., Reyes, J. M., and Rosenblatt, G., "Polaronic Hopping Conduction in Vanadium Phosphate Glasses," J. Appl. Phys., 42, 7, 2857-2864,(1971).

24. Novakov, T., "X-Ray Photoelectron Spectroscopy of Solids: Evidence of Band Structure," Physical Review B, 3, 8, 2693-2697, (1971).

25. Namrin, et al., "Valence Bands and Core Levels of the Isoelectronic Series LiF, BeO, BN, and Graphite Studied by ESCA," Phys. Scripta, 1, 277, (1970).

26. Ramquist, Lars., "Electronic Structure of Cubic Refractory Carbides," J. Appl. Phys., 12, 5, 2113-2120, (1971).

# PRE-SWITCHING AND POST-SWITCHING PHENOMENA

## IN AMORPHOUS SEMICONDUCTING

## FILMS

by

M. P. Shaw
Department of Electrical Engineering
Wayne State University
Detroit, Michigan 48202,

S. C. Moss*
Energy Conversion Devices, Inc.
Troy, Michigan 48084,

and

S. A. Kostylev** and L. H. Slack ***
Division of Minerals Engineering
Virginia Polytechnic Institute and
  State University
Blacksburg, Virginia 24061

## ABSTRACT

Low duty-cycle pulsed d.c. switching experiments have been performed on a variety of thin film Te-based semiconducting glasses. No premonitory effects are observed in the current-time profile of the non-switching OFF state. If, however, the threshold voltage is exceeded, a continuous current increase with time throughout the normal delay-time regime (pre-switching OFF state) is always observed prior to switching. In a given device or film this current rise is interrupted, independent of over-voltage, by the rapid switching transition at about the same relative current increment above the current background extrapolated to zero-time (leakage current). In the switched or ON (filamentary conduction) state the current level, as limited by the series load resistor, can determine the response of the device in the subsequent pre-switching OFF state. For loads in excess of $\sim 1k\Omega$, there is no effect on the pre-switching OFF state characteristics. For appreciably smaller loads, there is a continuous increase in delay time with increased pulse length (time spent in the previous ON state).

This letter describes some low duty-cycle pulsed d.c. switching experiments on thin film Te-based amorphous semiconductors. Our objective has been to characterize further the nature of the switching process, including the evolution of the filamentary ON state, and to demonstrate the influence of some simple circuit parameters such as the series load resistor, R, and pulse duration, $t_p$. "Ovonic" threshold switching[1] has been the subject of articles and review papers too numerous to reference properly. (The proceedings of the recent Fourth International Conference on Amorphous and Liquid Semiconductors[2] is an appropriate source.) The mechanism of switching is now being clarified as the distinctions among electro-thermal theories[3] and theories in which purely electr.c effects[4] dominate the switching transition become more clearly delineated. Our results should provide a further basis for distinguishing among these theories and determining the circumstances under which each may be applicable.

Thin films were prepared as follows to be compared with the experimental DO-7 threshold switches developed by Energy Conversion Devices, Inc.:

1. A homogeneous $As_{49}Te_{51}$ glass prepared from 99.999% pure elements was electron-beam evaporated onto either a brass foil or a metallographically polished Al plate coated with ~ 0.1 $\mu$m of Mo. These films were all 2 $\mu$m thick.

2. AsTe, $As_2Te_3$ and a few compositions in the Te-As-Si-Ge system were sputtered onto metallographically polished

plates of brass or Mo-coated Al (as above) in thicknesses of 0.5, 1.0 and 2.0 $\mu$m.

X-Ray diffraction patterns were taken to check the amorphous nature of the films.

Experiments were performed with $t_p$'s from 0.1 to 30 $\mu$sec applied at a pulse repetition frequency (PRF) of 50-1000 hz. Interpulse heating effects were negligible because of the long interpulse times. In a given experiment, the sample was considered to be the region of the film in the immediate vicinity of the copper or graphite counter-electrode. The copper electrode (~200 $\mu$m wide at the tip) made a larger area contact than the graphite. The counter-electrode was set and maintained under a slight constant pressure similar to that in the DO-7 package. [This device consists of two hemispherical graphite electrodes identical to the ones used here as counter-electrodes. The electrodes are each coated with an evaporated film of a Te-Se-S glass ~ 0.5 $\mu$m thick, held together under a slight pressure and hermetically sealed in a convenient package.] The measured low-voltage resistances of $As_{49}Te_{51}$ and AsTe films ranged from 10-50 k$\Omega$, the $As_2Te_3$ from 3-10 k$\Omega$ (these are on the edge of glass formation) and the Te-As-Si-Ge films from 100-500 k$\Omega$. All films contained many samples that demonstrated reproducible switching.

Fig. 1 shows the results of the evolution of current, I, with time in the DO-7 threshold switch. The low-current ohmic OFF state resistance of this device was ~2.4 M$\Omega$ and the steady state bias at threshold, $V_{th}$,

was ~ 27 volts. Of principal interest in Fig. 1 is the continuous rise in the pre-switching OFF state current up to the point of the switching transition. In this well-known "delay-time" regime, the delay time, $t_d$, decreases rapidly with increasing overvoltage (voltage in excess of $V_{th}$). In Fig. 1(a), the lowest I(t) profile (non-switching OFF state) shows a current that decreases very slightly with time. We attribute this fall primarily to the long relaxation tail of the initial displacement current spike that occurs upon application of the fast risetime voltage pulse. The important point is that in the absence of switching there is no premonitory rise in current. If there is a conductivity change due to uniform heating, it is completed in 1 $\mu$sec or less and the device achieves a uniform steady non-switching OFF state at all current levels below $V_{th}$. No evidence exists for the development of current density inhomogeneities, thermal or otherwise, in the non-switching regime.

Once the applied pulse exceeds $V_{th}$, however, quite the reverse is true. This can be clearly seen in the magnified current scale of Fig. 1(b). Following the capacitive discharge, all the pre-switching OFF state curves show an upward trend in current eventually terminating with the rapid vertical switching transition. Within our ability to detect it, the gradual current evolution begins approximately at the onset of the pulse, a point which we shall demonstrate more clearly with another sample. The conclusion seems inevitable, and is borne out by all our experiments performed at varying overvoltages on a variety of devices and thin film

41

sandwich structures, that $t_d$ is the time during which the eventual instability is forming. This is not surprising, and the ease with which the evolution of the filamentary instability can be observed should depend mainly on the spatial extent of this instability compared with the active area of the film. A rapidly evolving current density inhomogeneity (a nucleating filament, or growing filamentary plasma or collapsing electro-thermal filamentary column, etc.) will make its presence felt if the amount of current carrying or short circuiting that it performs is not negligible compared to the current flow through the rest of the device. If the evolving filament is very thin, it will be barely observable in the I(t) profile until it finally is fully established and the device switches. A wider lateral instability will be more readily observed as it forms. These ideas closely parallel those of Homma[5] concerning the development of observable electrical precursors to switching on the surface of an amorphous chalcogenide semiconductor.

To demonstrate the phenomenon discussed above in a more quantitative fashion, we show in Fig. 2 results of I(t) profiles taken on an AsTe film. Because of the lower resistivity of this glass, $V_{th}$ was just under 3.5 volts. Each curve in Fig. 2 represents a large number of oscilloscope traces of the type shown in Fig. 1 but with much higher current levels both because of the lower resistivity and because of the larger area contact of the copper counter-electrode. [Because copper eventually alloys with the Te-based glass and promotes its crystallization, sample lifetimes with the brass and copper systems were much shorter than with the graphite –

Mo(Al) combination.] These higher current levels and differing boundary conditions from the DO-7 configuration permitted a much more careful determination of the I(t) curves, especially in the vicinity of the zero-time point. The averages of several I(t) profiles were plotted on a log-log scale to test for power law behavior and two distinct dependences were seen at each overvoltage. The time dependence of the current growth followed the general form $I = At^{n_1} + Bt^{n_2}$, where A and B are constants. $n_1$ was in the range 1-3 and increased with increasing overvoltage. $n_2$ was roughly 9 and appeared not to depend on voltage in any systematic way. The transition point between the two dependences, which we call the threshold current, $I_{th}$, increased with increasing overvoltage, especially when the zero time (leakage) current was not subtracted. The speed, $t_d$, and spatial extent with which the threshold instability develops (the smaller $n_1$, the less the lateral extent of the growing instability) depend strongly on overvoltage and are measures of how high the device is biased. At any given overvoltage, threshold occurs at about the current $I_{th} = I_o \times (const.)$ where $I_o$ is the current extrapolated to zero time and the constant is independent of overvoltage.

The post-switching behavior of these films, including the nature of the filamentary ON state and the temperature levels achieved during and after switching, (especially as they relate to the question of the "forming"[6] of a switching device) is also of great interest. As described recently by Coward[6], it is well-known that Ovonic threshold switches have a first-fire or break-in voltage at threshold that is substantially greater than the running threshold that obtains after several cycles of operation. Most

43

likely among the causes of both the large first-fire voltage and the subsequent locating or pinning of a higher conductivity filamentary region in a formed device are:

1)  Healing of a dirty or imperfect electrical contact at the glass-electrode interface. This may always be an important component of the first-fire effect.

2)  Electromigration in the filamentary region which produces a crystalline pedestal shortening the glassy portion of the device. This would usually be limited by the ensuing back diffusional gradient that is simultaneously established[7] if solute cannot easily flow laterally into the filamentary column. a.c. operation of a device would tend to form and dissolve such a pedestal on successive switchings.

3)  Interfacial crystallization at the electrodes due to the eventual development in the ON state of most of the voltage drop in the vicinity of the electrodes. In electronic models of switching, most of the joule heating would take place at the electrodes[8]. In an electro-thermal model, there would be an abrupt temperature decrease at the electrodes[3] which might provide the appropriate boundary condition for heterogeneous nucleation. Electro-thermal arguments that might lead to a crystallization front limited to the vicinity of the electrode under continuous operation are, however, somewhat tortuous.

To test these ideas, the data in Fig. 3 were collected for a Te-As-Si-Ge film over Mo with a graphite counter electrode. The qualitative results were again independent of the substrate and counter-electrode and were reproducibly and reversibly obtained with most of the samples. Fig. 3(a) demonstrates the dependence of $t_d$ on $t_p$ at fixed overvoltage. With the larger R there is no dependence. With $100\,\Omega$, however, there is a steady increase in $t_d$ as the device is left for longer periods of time in the ON state (longer $t_p$). This indicates that if the filamentary conducting material is left in the ON state at a low current level (large R, low power dissipation), there is no alteration of the "formed" conducting path. Once formed, it remains so with a well-defined $V_{th}$ which is lower than the surrounding glass and does not decrease continuously with cycling. However, if the power dissipation in the ON state is increased by decreasing R, it is our opinion that the filamentary region spreads, the temperature rises at the higher current levels, and the filamentary region is rehomogenized. The crystalline interfacial material (or pedestal) is thus remelted, or redissolved, and requenched as a glass. $V_{th}$ is thereby raised in this up-quench and down-quench treatment and the device is returned to a more nearly virgin state. Figure 3(b) shows the partial recovery of the virgin $V_{th}$ under fixed $t_p$. This figure also clearly demonstrates the dependence of $t_d$ on overvoltage. Because the threshold is raised for $R = 100\,\Omega$, the applied voltage represents a substantially reduced overvoltage and $t_d$ is consequently increased.

The results shown in Fig. 3 are reversible. By increasing R or decreasing $t_p$, $t_d$ gradually decreases as the running threshold again drops. Increasing $t_p$ again (or decreasing R) will then restore the higher $V_{th}$'s and longer $t_d$'s. This process naturally cannot usually be repeated indefinitely because the high current levels with $R = 100\,\Omega$ eventually degrade the device.

In summary, our experiments elucidate both the development of the filamentary instability in the pre-switching OFF regime - it starts approximately at zero time for any overvoltage - and the nature of the forming or breaking-in process in the post-switching portion of the I-V curve. An important consequence of the filament forming process is that it represents a favored area for subsequent threshold switching. This means that the developing instability has a lateral extent which may be comparable with this favored area, thus rendering it visible throughout the delay time period.

---

**Visiting scientist at Virginia Polytechnic Institute and Wayne State University under the auspices of the National Academy of Sciences. Permanent address, Department of Semiconductor Electronics, Institute of Mechanics and Academy of Sciences of the Ukraine, Lesco-Popelya St. 9, Dnepropetrovsk, 320005, U.S.S.R.
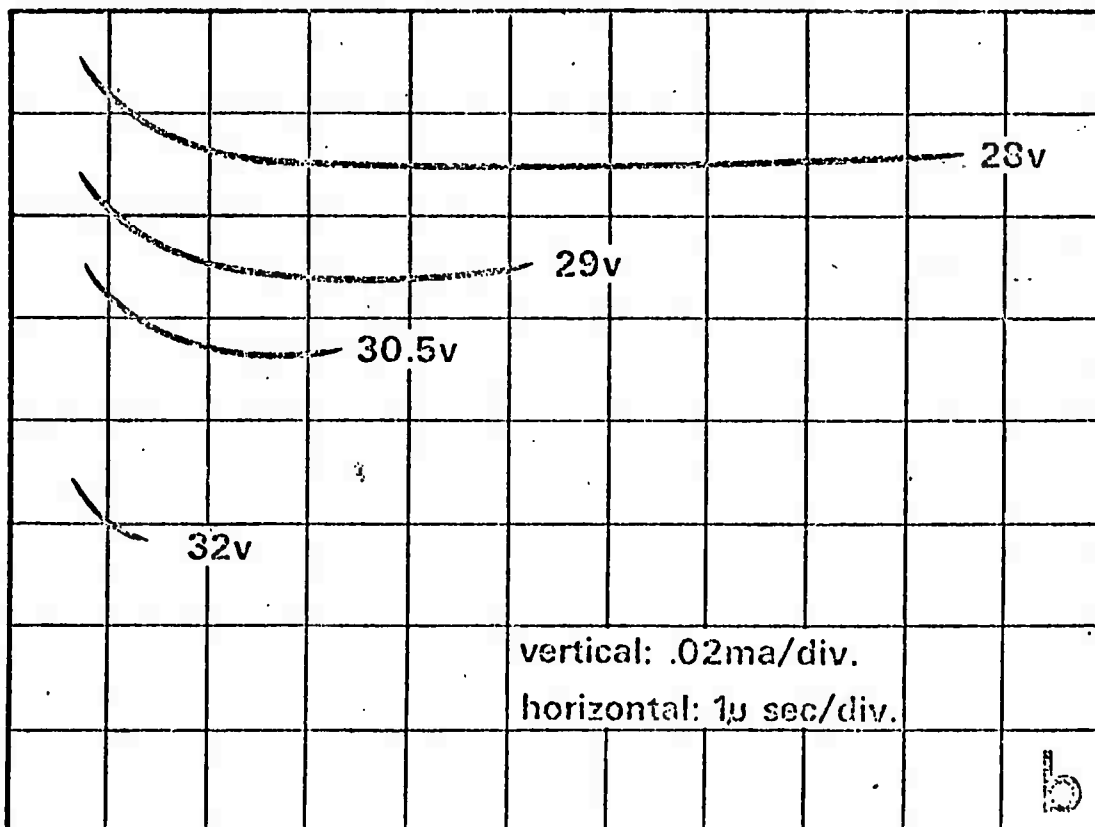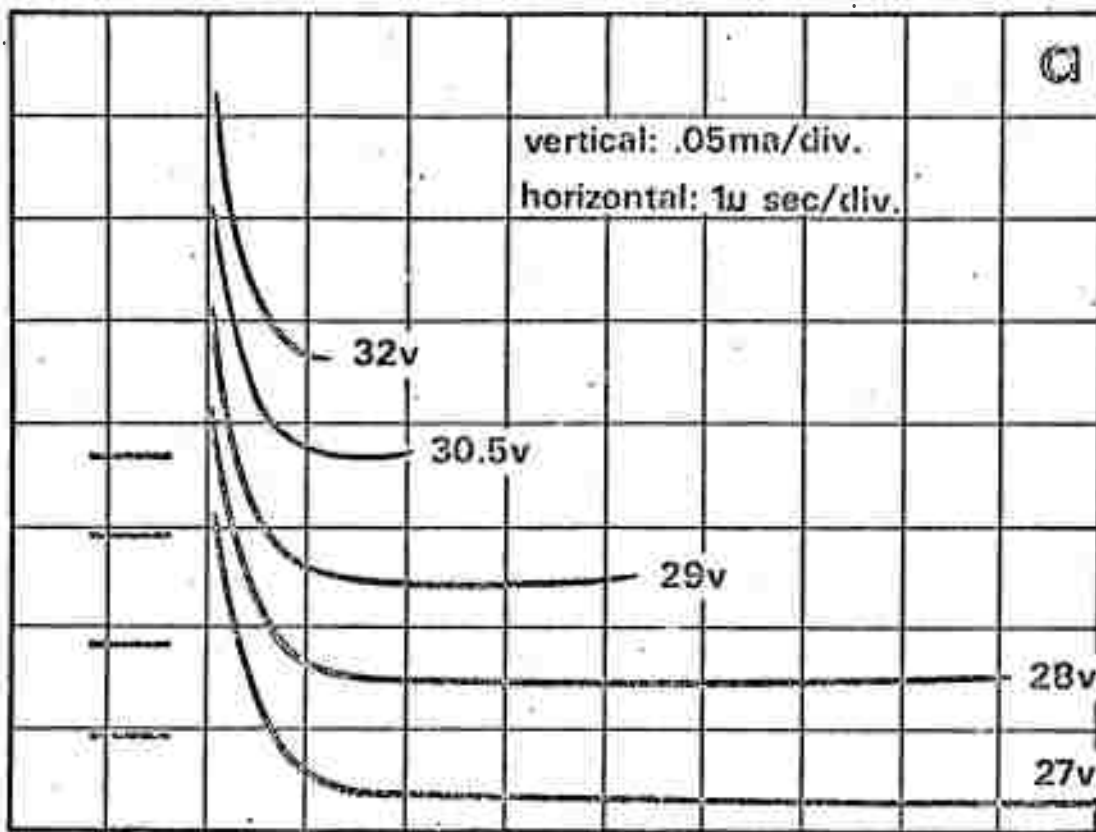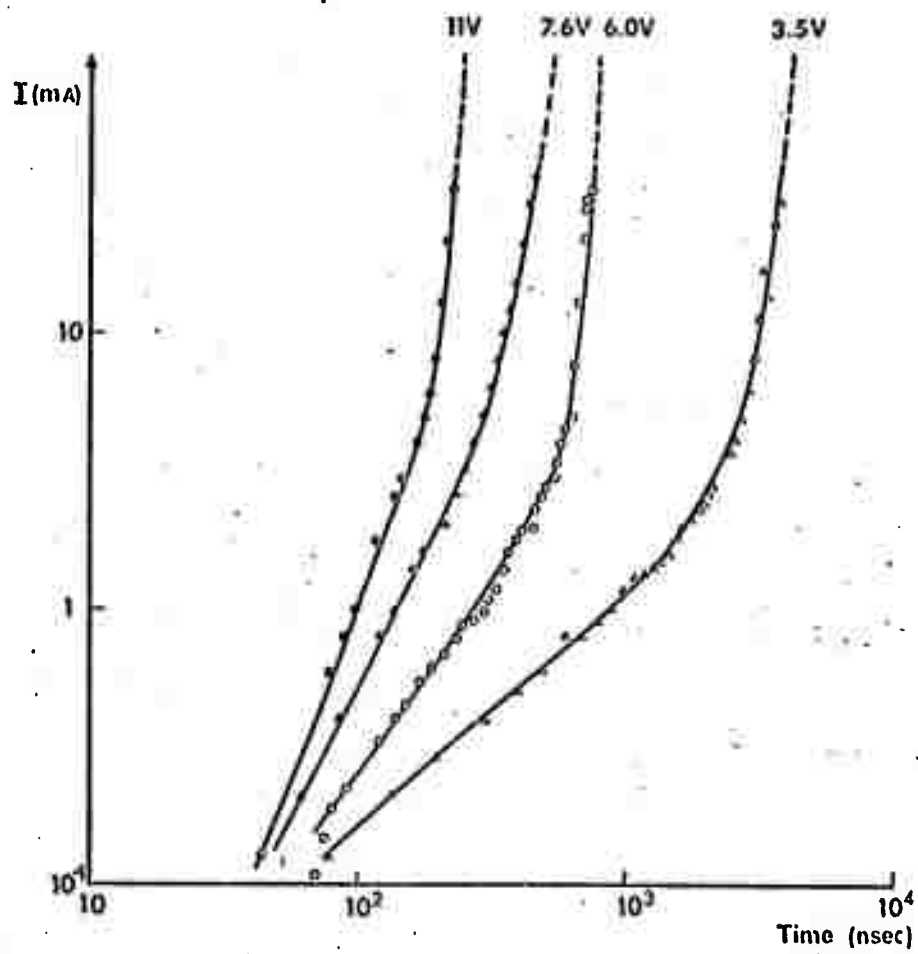
## REFERENCES

1. For a recent discussion of switching in amorphous semiconductors, see H. Fritzsche, Proc. Second Int. Conf. on Conduction in Low Mobility Materials, (Taylor & Francis Ltd., London 1971) p. 279. For a general review of switching in solids, see N. Klein, Thin Solid Films 7, 149 (1971) and C. N. Berglund and N. Klein, Proc. IEEE 59, 1099 (1971). For a comprehensive review of the field of amorphous semi-conductors, see D. Adler, Critical Reviews in Solid State Sciences 2, 317 (Chem. Rubber Pub. Co., Cleveland, Ohio 1971).

2. Proc. Fourth Int. Conf. Amorph. and Liq. Semiconductors (Aug. 1971), J. Non-Cryst. Solids 8-10 (1972), in press.

3. See, e.g., T. Kaplan and D. Adler, Appl. Phys. Lett. 19 418 (1971) and Proc. Fourth Int. Conf. Amorph. and Liq. Semiconductors, J. Non-Cryst. Solids 8-10 (1972), in press.

4. See e.g., W. van Roosbroeck and H. C. Casey, Jr., Phys. Rev. 5B, 2154 (1972); and W. van Roosbroeck, Phys. Rev. Lett. 28, 1120 (1972).

5. K. Homma, Appl. Phys. Lett. 18, 198 (1971).

6. L. A. Coward, J. Non-Cryst. Solids 6, 107 (1971).

7. E. J. Evans, Proc. Fourth Int. Conf. Amorph. and Liq. Semiconductors, J. Non-Cryst. Solids 8-10 (1972), in press.

8. Thermal switching in an avalanching diode can also be initiated at an electrode. See, e.g., R. A. Sunshine and M. A. Lampert, Appl. Phys. Lett. 18, 468 (1971).

## FIGURE CAPTIONS

Figure 1      Current vs. time, I(t), for a DO-7 device. The zero-voltage base lines are on the left in (a) and the vanishing of the trace on the right in (a) and (b) corresponds to the occurrence of switching. $R = 2$ k$\Omega$, $t_p = 30$ $\mu$sec, PRF = 30 hz. Each trace corresponds to a different applied voltage.

a) The lowest trace is 27 volts (non-switching OFF state) and the succeeding traces result for voltages increased up to 32 volts. Horiz. = 1 $\mu$sec/div. Vert. = 0.05 ma/div.

b) The top trace is 28 volts and the succeeding traces again represent increased voltages above threshold. Horiz. = 1 $u$sec/div. Vert. = 0.02 ma/div. Note especially the positive slope of I(t) at 28 and 29 volts.

Figure 2      Current rise with time during a switching mode in a 2$\mu$m thick AsTe film on a brass substrate using a copper counter-electrode. $R = 1$ k$\Omega$. 3.5V is the d.c. threshold voltage.

Figure 3      a) $t_d$ vs. $t_p$ at two different R's for a Te-As-Si-Ge film. The data were taken with a PRF - 50 hz and a bias of 22 volts, starting at the shortest $t_p$. When the large R data is taken starting with a long pulse, $t_d$ <u>decreases</u> slightly as $t_p$ increases. This feature is not completely understood.
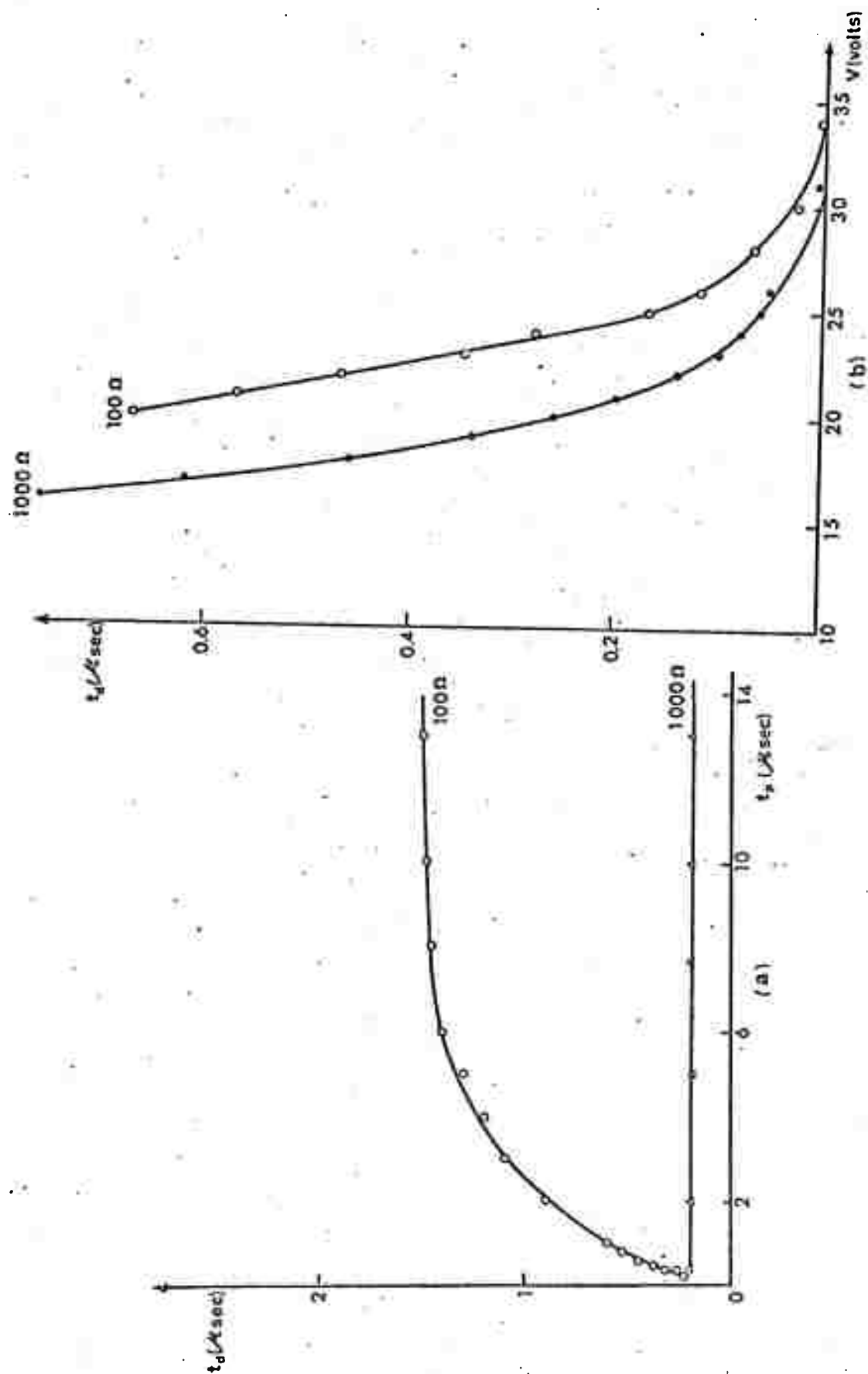
b) $t_d$ vs. V at two different R's with $t_p = 1 u$sec.

vertical: .05ma/div.
horizontal: 1μ sec/div.

32v
30.5v
29v
28v
27v



28v
29v
30.5v
32v

vertical: .02ma/div.
horizontal: 1μ sec/div.

49

Fig.3